PROTEIN INTERACTIONS OF GTP-ase OF IMMUNITY ASSOCIATED PROTEIN 3

Pilvi Ruotsalainen

Master's Thesis

University of Jyväskylä

Department of Biological and Environmental Science

Cell and molecular biology

03.09.2014

PREFACE

This study was carried out at Biomedicum Helsinki, Research Programm of Molecular Neurology, University of Helsinki during summer and fall 2010. The thesis was written during the long years 2011-2014.

I am grateful to my supervisor Dr. Brendan Battersby for the opportunity to work in his research group under his patient and encouraging guidance. I learned plenty that will help me in years to come. I also want to thank other members of our group, Heidi, Maarit, Nick, Paula, Riikka, Taina and Uwe, for being supportive and making the atmosphere in our group so friendly and cheerful. In addition I want to thank all members of Anu Wartiovaara's group for the support and help, not to forget the hilarious moments outside the lab. Thank you all for the many great memories and experiences filled with laughter! I also deeply appreciate the help of Tuula Nyman, who performed the mass spectrometry studies and guided me to understand the wonders of mass spectrometry analysis. Lastly I'm extremely grateful for you Nadine that you found time to proof-read and help me to improve my thesis. Your advices were irreplaceable!

Lopuksi haluan kiittää koko perhettäni kaikesta tuesta ja avusta kaikkien näiden vuosien ajan. Viimeisimpänä muttei ehdottomasti vähäisimpänä, haluan kiittää rakkaita ystäviäni mahtavista yhteisistä hetkistä vuosien varrella. Ilman niitä olisi ollut väritöntä. Erityisesti haluan kiittää Juulia, Niinaa ja Jenniä avustanne gradun kanssa. Niiden miljoonien keskustelujen, apunne ja tukenne avulla tämä on vihdoin valmis. Tästä alkakoon uusi elämän vaihe.

Jyväskylässä kesällä 2014

University of Jyväskylä
Faculty of Mathematics and Science

Abstract of Master´s Thesis

Author: Pilvi Ruotsalainen
Title of thesis: Protein interactions of GTP-ase of immunity associated protein 3
Finnish title: Vastustuskykyyn vaikuttavan GTPaasi 3:n proteiini-interaktiot
Date: 03.09.2014 **Pages:** 50+8

Department: Department of Biological and Environmental Science
Chair: Cell and Molecular Biology
Supervisor(s): Ph.D. Brendan Battersby

Abstract:

The protein family GTP-ase of immunity associated protein (Gimap) is expressed in all vertebrates and angiosperm plants. One member of this family, *Gimap3*, is a pseudogene in humans but is expressed in mice, mainly in immune tissues and leukocytes. Together with members of the Bcl-2 family, *Gimap3* and its paralogue, *Gimap5*, are needed for the maturation and survival of T cells as well as the maintenance of T cell homeostasis. However the mechanisms underlying this process are still unknown. Autophagy-related protein 5 (Atg5), a component of the autophagy degradation system, also plays a role in T cell maturation, especially in the negative and positive selection of T cells. Preliminary genetic studies suggested that the stability of Gimap3 is dependent on the expression of Atg5 but, whether they interact directly, remains to be seen.

Furthermore *Gimap3* is the first nuclear gene shown to modify the segregation of mitochondrial DNA (mtDNA) in hematopoietic tissues, although through an unknown mechanism. The morphological changes of mitochondria through fission and fusion are also connected to the maintenance and inheritance of mitochondria and possibly also to the segregation of the mitochondrial genome. Pathogenic mutant mtDNA variants in somatic tissues are shown to affect the segregation pattern, which is linked to the severity and the onset of mitochondrial disorders. Therefore, understanding the mechanism of mtDNA segregation is critical for understanding the development of mitochondrial disorders.

In this thesis, a co-immunoprecipitation protocol was optimized to study the protein interactions of Gimap3 in order to elucidate how Gimap3 functions in maturation and development of T lymphocytes and also, by what mechanism it modifies the segregation of mtDNA. To achieve reliable results, an antibody precipitating Gimap3 specifically and efficiently, and a detergent with good solubilization capacity were chosen. The background contaminants in elution were reduced by differential centrifugation and stringent washes. Due to the high levels of background contamination, preliminary crosslinking experiments were done to further decrease the background with even more stringent washes. In mass spectrometry analysis, one protein, vesicle trafficking protein SEC22b (SEC22b), was identified to potentially interact with transmembrane domain of Gimap3. Atg5 was not found to interact with Gimap3 in the conditions tested. Further studies are needed to confirm these results and to optimize the co-immmunoprecipitation method for full-length Gimap3 in order to discover more protein interactions as well as interactions with its N-terminus.

Keywords: Gimap3, protein-protein interactions, T cell maturation, mtDNA segregation

Jyväskylän yliopisto **Pro gradu –tutkielman tiivistelmä**
Matemaattis-luonnontieteellinen tiedekunta

Tekijä: Pilvi Ruotsalainen
Tutkielman nimi: Vastustuskykyyn vaikuttavan GTPaasi 3:n proteiini-interaktiot
English title: Protein interactions of GTP-ase of immunity associated protein 3
Päivämäärä: 03.09.2014 **Sivumäärä:** 50+8

Laitos: Bio- ja ympäristötieteiden laitos
Oppiaine: Solu- ja molekyylibiologia
Tutkielman ohjaaja(t): FT Brendan Battersby

Tiivistelmä:

Vastustuskykyyn vaikuttava GTPaasi (Gimap) perheen geenejä ilmennetään kaikissa selkärankaisissa ja siemenkasveissa. Tämän proteiiniperheen jäsen, *Gimap3*, on ihmisissä valegeeni, mutta ilmenee hiirissä, pääosin periferaalisissa immunokudoksissa ja T-soluissa. Yhdessä Bcl-2 proteiiniperheen kanssa, *Gimap3* ja sen paralogi *Gimap5*, vaikuttavat T-solujen homeostasiaan säätelemällä niiden kypsymistä ja eloonjäämistä. Säätelymekanismia ei kuitenkin tällä hetkellä tunneta. Autofagosytoosissa tärkeässä osassa oleva autofagosytoosin kaltainen proteiini 5 (Atg5), vaikuttaa myös T-solujen kypsymiseen, erityisesti T-solujen negatiiviseen ja positiiviseen valintaan. Alustavat geneettiset tutkimukset ovat osoittaneet Atg5:n mahdollisesti säätelevän Gimap3:n stabiilisuutta solussa, mutta toistaiseksi proteiinien ei ole osoitettu olevan keskenään interaktiossa.

Gimap3 on myös ensimmäinen tuman geeni, jonka on todistettu vaikuttavan mitokondriaalisen DNA:n segregaatioon. Mitokondrioiden morfologisten muutosten on myös havaittu vaikuttavan mitokondrioiden periytymiseen ja homeostasiaan, mahdollisesti myös mitokondrion genomin segregaatioon. Segregaation mekanismin ymmärtäminen olisi tärkeää, koska mitokondriaalisten patogeenisten mutaatioiden on huomattu vaikuttavan segregaatioon, joka edelleen vaikuttaa mitokondriaalisen sairauden puhkeamiseen ja vaikeusasteeseen. Näin ollen segregaation mekanismin tunteminen auttaisi mitokondriaalisten sairauksien hallinnassa ja hoidossa.

Tässä työssä optimoitiin immuunisaostus-menetelmä Gimap3:n kanssa vuorovaikutuksessa olevien proteiinien määrittämiseksi. Näiden proteiini-vuorovaikutusten avulla mekanismit, joilla Gimap3 vaikuttaa T-solujen kypsymiseen sekä mitokondriaalisen DNA:n segregaatioon, selviäisivät. Luotettavien tulosten saamiseksi optimaalisen detergentin lisäksi varmistettiin vasta-aineen spesifisyys ja saostustehokkuus. Eluution taustaa vähennettiin erotus-sentrifugoinnilla sekä korkea suolapitoisilla pesuilla. Tämä ei kuitenkaan riittänyt, joten vielä korkeampi suolapitoisten pesujen käyttöä varten optimoitiin menetelmä proteiini vuorovaikutusten vakauttamiseksi kemiallisilla linkittäjillä. Massaspektrometri-tutkimuksessa vesikkeli-kuljetus proteiini SEC22b löydettiin olevan mahdollisesti vuorovaikutuksessa Gimap3:n kalvoa läpäisevän osan kanssa. Atg5:n ei havaittu olevan vuorovaikutuksessa Gimap3:n kanssa. Lisää kokeita tarvitaan näiden proteiinien vuorovaikutuksen varmistamiseksi sekä saostus-menetelmän optimoimiseksi kokopitkälle Gimap3:lle, jotta lisää vuorovaikutuksessa olevia proteiineja löydetään, myös N-terminaalisia proteiini-vuorovaikutuksia.

Avainsanat: Gimap3, proteiinien väliset vuorovaikutuset, T-solujen kypsyminen, mtDNA:n segregaatio

TABLE OF CONTENTS

PREFACE

ABSTRACT

TIIVISTELMÄ

TABLE OF CONTENTS

ABBREVIATIONS

1 INTRODUCTION 8

1.1 GTPase of immunity associated protein family 8

1.1.1 The structure and function of GTPase of immunity-associated protein family 8

1.1.2 GTPase of immunity-associated protein 3 and 5 9

1.2 Maturation of T lymphocytes and maintenance of their homeostasis 10

1.2.1 GTPase of immunity-associated protein 3 and 5 in maturation of T lymphocytes 11

1.2.2 Hetero-oligomerization potentially regulates the protein interactions of GTPase of immunity-associated proteins 12

1.2.3 Autophagy-related protein 5 in adaptive immunity 14

1.3 Inheritance and segregation of mitochondrial DNA 15

1.3.1 Segregation of mitochondrial DNA under nuclear control 15

1.3.2 Morphological changes of mitochondria influence the maintenance and segregation of mitochondrial DNA 16

1.3.2.1 A membrane tethering protein complex affects the maintenance and segregation of mitochondrial DNA 17

2 AIM OF THE STUDY 18

3 MATERIALS AND METHODS 19

3.1 Retroviral expression and cell culture 19

3.2 Homogenization and differential centrifugation 19

3.3 Co-immunoprecipitation 20
3.4 Trichloroacetic acid-precipitation 21
3.5 Immunoblotting and silverstaining 22
3.6 Mass spectrometry analysis 23
3.7 Crosslinking experiments 23

4 RESULTS 24
4.1 Anti-HA antibody precipitated the bait protein specifically and efficiently 24
4.2 Enrichment of bait protein by differential centrifugation 25
4.3 The balance between good recovery of bait protein and the amount of background contaminations in the elution was optimal with *n*-dodecyl β-D-maltoside 26
4.3.1 Increasing the recovery of bait protein in the elution 29
4.4 Identification of interacting proteins by mass spectrometry 29
4.4.1 Identified interaction partners 30
4.5 The crosslinking of the bait protein 31
4.5.1 Co-immunoprecipitation of crosslinked bait protein was unsuccessful 32

5 DISCUSSION 34
5.1 Optimization of co-immunoprecipitation 34
5.1.1 Determining the antibody specificity and precipitation efficiency 34
5.1.2 An optimal detergent with good protein solubilization efficiency 35
5.1.3 Reduction of background in the elution 38
5.1.4 Identification of interaction partners by mass spectrometry 40

6 REFERENCES 44

APPENDICES 51

ABBREVIATIONS

Atg5= Autophagy-related protein 5

CMC= critical micelle concentration

co-IP= co-immunoprecipitation

DC= differential centrifugation

DDM= *n*-dodecyl β-D-maltoside

DFDNB= 1,5-difluoro-2,4-dinitrobenzene

DSG= disuccinimidyl glutarate

DSP= dithiobis[succinimidylpropionate]

E= elution sample of co-IP

ER= endoplasmic reticulum

ERMES= ER-Mitochondria Encounter Structure (protein complex)

FT= flow-through sample of co-IP

GFP-(261-301)Gimap3= the green fluorescent protein (GFP)-tagged transmembrane domain (261-301) of Gimap3

Gimap= mouse GTPase of immunity-associated protein

GIMAP= human GTPase of immunity-associated protein

HA= human influenza hemagglutinin tag

HMP= heavy membrane pellet

LMP=light membrane pellet

MHC= major histocompatibility complex

mtDNA= mitochondrial DNA

NP=nuclear pellet

SEC22b= vesicle trafficking protein SEC22b

SM-1= starting material after homogenization

SM-2= starting material from HMP sample

STDC= sodium taurodeoxycholate hydrate

TCR= T cell receptor

W= wash sample of co-IP

1 INTRODUCTION

1.1 GTPase of immunity associated protein family

GTPase of immunity-associated proteins (Gimap), also known as immune-associated nucleotide-binding proteins (IANs), belong to the clade of guanine nucleotide-binding (G) proteins, and were first identified by induced expression in *Arabidopsis thaliana* infected with *Pseudomonas syringae* (Reuber and Ausubel, 1996; Poirier et al., 1999). Besides angiosperm plant genomes, the protein family is expressed in all vertebrate genomes but not in invertebrates or unicellular cells (Poirier et al., 1999; Krücken et al., 2004).

Humans have a 300 kb *GIMAP* gene cluster on chrosome 7q36.1 containing seven functional *GIMAP* genes. In mice, the gene cluster is located on the chromosome 6 and shows similar proximal to distal arrangement and orientation as in humans (Daheron et al., 2001; MacMurray et al., 2002; Krücken et al., 2004). In mammals, *Gimaps* are mostly expressed in hematopoietic tissues, such as the spleen and lymph nodes and also, to some extent in immune cells. An exception is *GIMAP4,* which is highly expressed in non-immune tissues such as the placenta, prostate and testis (Krücken et al., 2004).

1.1.1 The structure and function of GTPase of immunity-associated protein family

The characteristic feature of Gimaps is their N-terminal AIG1 domain which consists of five GTP-binding motifs, also called G-motifs (G1-G5) (Daheron et al., 2001; Krücken et al., 2004). The conserved box, between motifs G3 and G4, is highly hydrophobic and predicted to form an extended sheet secondary structure surrounded by random coiled regions (Krücken et al., 2004). The coiled-coil domains precede the transmembrane domain (60-130 amino acids long) in the C-terminus (Krücken et al., 2004; Nitta et al., 2006; Schwefel et al., 2010). Some Gimaps have hydrophobic segments in the

transmembrane domain which is suggested to work as a transmembrane anchor (Daheron et al., 2001; Krücken et al., 2004; Schwefel et al., 2010).

GIMAPs are believed to function as a cross-linker between different lipid droplets or source membranes. They might also work as a scaffold protein, assembling the interaction partners on the membrane or modelling the membranes (Schwefel et al., 2010; for review see Jokinen et al., 2011). All these hypotheses are supported by the localization of GIMAPs to the membrane compartments and their structure and oligomerization mechanism (Daheron et al., 2001; Schwefel et al., 2010; Wong et al., 2010). The dimerization of GIMAP2 in a nucleotide-dependent manner via two interfaces results in a dimer with the C-terminal transmembrane domains pointing in opposite directions. This would enable the crosslinking of two distinct membranes, for example endoplasmic reticulum (ER) and mitochondria (Schwefel et al., 2010).

1.1.2 GTPase of immunity-associated protein 3 and 5

GTPase of immunity-associated protein 3 (Gimap3), also known as immune-associated binding protein 4 (IAN4), was discovered through its induced expression in a response to *Bcl/Abl* oncogene in myeloma cells (Daheron et al., 2001; Nitta et al., 2006). Although a functional gene in mice, *GIMAP3* is a pseudogene in humans due to a frameshift mutation, which results in premature termination (Krücken et al., 2004). The mouse *Gimap3* has two open reading frames (ORF), the upstream ORF consists of 67 codons and the second ORF encodes a protein of 301 amino acids (Daheron et al., 2001).

Gimap5, the paralogue of *Gimap3,* was first identified in the BioBreeding rat (BB-rat), when a frameshift deletion caused T cell lymphopenia eventually leading to diabetes (Macmurray et al., 2002). In mice, the shared homology with *Gimap3* is 83,8% in amino acid and 88,9% in nucleotide sequences (Nitta et al., 2006). In humans, *GIMAP5* has two splice variants encoding two protein products: a major splice product of 307 amino acids, and a second of 347 amino acids (Krücken et al., 2004). In mice, *Gimap3* is only expressed in immune tissues and leukocytes (Daheron et al., 2001; Jokinen et al., 2010), whereas

Gimap5 is expressed ubiquitously, yet mainly in the spleen and lymph nodes (Krücken et al., 2004).

Gimap3 and Gimap5 share the characteristic features of Gimap proteins with GTP-binding ability and both have hydrophobic transmembrane domains in the C-terminus (Fig. 1), which is necessary for anchoring the protein to a membrane (Daheron et al., 2001; Krücken et al., 2004). The localization of both Gimap3 and Gimap5 is controversial. Previous localization studies have been based on the over-expression of these proteins, which may have caused mislocalizatioin artifacts. In these studies, Gimap3 was shown to localize to the outer membrane of mitochondria and Gimap5 to the Golgi apparatus, centrosome and ER in addition to mitochondria (Daheron et al., 2001; Sandal et al., 2003; Zenz et al., 2004; Nitta et al., 2006; Dalberg et al., 2007). In the latest studies, endogenously expressed GIMAP5 was shown to localize to lysosomes and multivesicular bodies in lymphoid cells (Wong et al., 2010). Also, the Battersby group has had several encouraging results showing that stably expressed Gimap3 localizes to the ER membrane network (unpublished data).

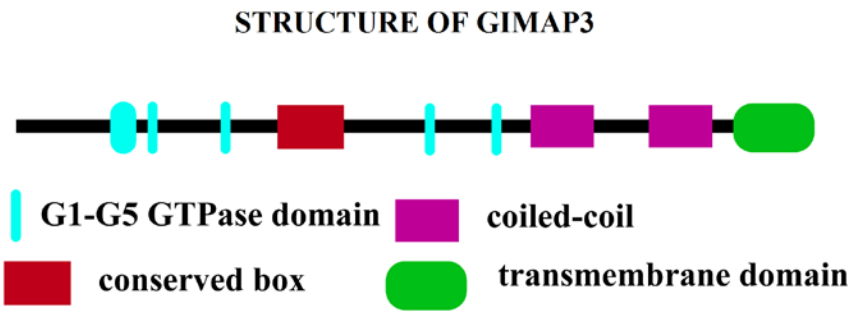

Figure 1: Structure of Gimap3. The Gimap3 structure consists of five GTPase domains and a conserved box, which together form the AIG1 domain, characteristic of the Gimap family. The coiled-coil domain is adjacent to the transmembrane domain in the C-terminus. Gimap3 is anchored to the membrane through its transmembrane domain.

1.2 Maturation of T lymphocytes and maintenance of their homeostasis

The maturation of T lymphocytes in the thymus includes several checkpoints to prevent generation of T cells with a nonfunctional or autoreactive T cell receptor (TCR) complex. During the first checkpoint, called β selection, the immature $CD4^-$ $CD8^-$ double-negative

(DN) cells with the right rearrangement of TCRβ chain are selected for further differentiation to CD4 CD8 double positive (DP) cells (Fig. 2) (Dudley et al., 1994; von Boehmer et al., 1999). This is followed by the second checkpoint, where the $CD4^+$ $CD8^+$ DP cells undergo positive and negative selection signaling through the TCR complex, generating mature major histocompatibility complex (MHC)-restricted, self-tolerant single positive (SP) $CD4^+$ and $CD8^+$ T lymphocytes, that are released to the peripherial lymphoid organs (Fig. 2) (for review see Boyman et al., 2012).

The maturation of T lymphocytes in the thymus and the maintenance of their homeostasis in the periphery are dependent on the same survival factors: interaction of TCR complex with the MHC complex and IL-7 cytokine binding to the cytokine receptor. Both TCR complex and cytokine receptor activate intracellular signal transduction molecules, which results in the increased expression of anti-apoptotic (e.g., Bcl-2) and decreased expression of pro-apoptotic molecules (e.g., Bim, Bax, Bad), preventing the apoptosis of the cell (Veis et al., 1993; Kimura et al., 2013).

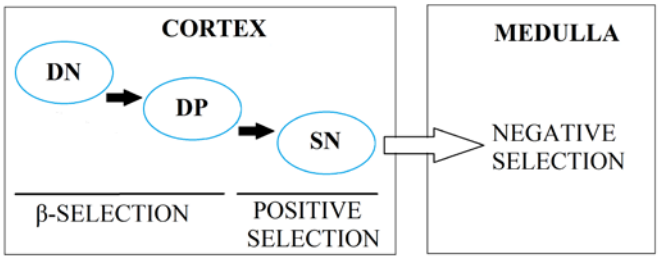

Figure 2: Maturation of T cells in the thymus. The lymphoid progenitor cells, migrated from bone marrow to the cortex of thymus, develop during β-selection from immature $CD4^-$ $CD8^-$ double negative (DN) T cells into $CD4^+$ $CD8^+$ double positive (DP) T cells, which have the re-arrenged TCRβ chain. In positive selection, DP cells with functional TCR complex mature into $CD4^+$ or $CD8^+$ single positive (SN) T cells, which migrate to the medulla of thymus. There the T cells undergo negative selection, in which the self-reactive T cells die by apoptosis and the self-tolerant T cells are released to the peripherial immune tissues (figure modified from Xu et al., 2013) (Dudley et al., 1994; for review see Xu et al., 2013).

1.2.1 GTPase of immunity-associated protein 3 and 5 in maturation of T lymphocytes

Gimaps have been shown to take part in the selection, survival and apoptosis of T-cell development, as well as their homeostasis (Nitta et al., 2006; Dalberg et al., 2007). During

the positive selection of T cell maturation from DP ($CD8^+$ $CD4^+$) into SP thymocytes ($CD4^+$ or $CD8^+$), the expression of both *Gimap3* and *Gimap5* is increased (Nitta et al., 2006). In spite of the similar gene expression pattern, they act at different stages of T cell maturation. The knockdown of *Gimap3* by shRNA disrupted T cell maturation at the stage of the positive selection of SP thymocytes and also decreased their cellularity, whereas the *Gimap5* knockdown combined with withdrawal of interleukin-2 caused enhanced apoptosis of DP thymocytes decreasing their cellularity at earlier stages. Both studies of T-lymphopenia in the BB-rat and *Gimap5* knockout mice showed *Gimap5* to be also essential for the survival of immature and mature T lymphocytes in the peripherial immune tissue by preventing premature cell death (MacMurray et al., 2002; Nitta et al., 2006; Schulteis et al., 2008; Barnes et al., 2010).

The latest studies with *Gimap3*$^{-/-}$ *Gimap5*$^{-/-}$ mice have shown *Gimap3* to maintain homeostasis of mature T lymphocytes in peripheral immune tissues as well. The deficiency of *Gimap3* enhanced the impact of *Gimap5* deficiency leading to a decrease of both peripheral CD4+ and CD8+ T-cell populations. This impaired survival was linked to the reduced expression of anti-apoptotic Bcl-2 and Bcl-X_L but whether Gimap3 and 5 regulate expression of these anti-apoptotic molecules or act posttranslationally is not known (Yano et al. 2014). In addition, Gimaps are linked to the progression of leukemogenesis and the development of autoimmune diseases, as *Gimap5* was shown to regulate T- regulatory cell differentiation or activity by activating Foxo1 and Foxo3 transcription factors needed for the expression of T regulatory cell regulator, Foxp3 (for review see Nitta and Takahama 2007; Aksoylar et al., 2012; Yano et al. 2014).

1.2.2 Hetero-oligomerization potentially regulates the protein interactions of GTPase of immunity-associated proteins

The similar gene expression pattern of *Gimap3, Gimap5* and *Bcl-2* during positive selection of T cells and interaction between Gimap3 and Gimap5 with both anti-apoptotic and pro-apoptotic members of the Bcl-2 family support the hypothesis that they regulate together T lymphocyte survival and maturation in mice. However, their mechanisms of

action remain largely unknown (Veis et al., 1993; Nitta et al., 2006; Yano et al., 2014). Oligomerization studies of GIMAP2 and GIMAP7 have shed light on the regulation mechanism of protein interactions involving GIMAPs (Schwefel et al., 2010; Schwefel et al., 2013).

Recent studies have shown that the GTPase activity of the GIMAP family appears to be controlled by hetero- and homodimerization. Whereas a homodimer of GIMAP2 was unable to hydrolyze GTP on its own, hetero-oligomerization with GIMAP7 stimulated GTP hydrolysis. GTP hydrolysis of GIMAP2-GIMAP7 heterodimer occurred following an analogous mechanism as with a GIMAP7 homodimer: the helical extension of a conserved argigine from conserved box of GIMAP7 protruded to the opposing GIMAP2 monomer and hydrolyzed GTP to GDP. The heterodimerization hypothesis was supported by the co-localization of these GIMAPs to lipid droplet-like structures in cells. This led to formulate a regulation mechanism where GIMAPs, devoid of transmembrane domain, are mobile and as catalytically active, can dimerize and stimulate GTP hydrolysis of catalytically inactive and immobile GIMAPs that are anchored to the membranes via the C-terminal transmembrane domain. After GTP hydrolysis GIMAPs would be in a GDP-bound form and GIMAP scaffolds are thought to disassemble and unable to bind other interacting proteins (Schwefel et al., 2010; Schwefel et al., 2013).

The close relatedness of GIMAP4 to GIMAP7 and their similar GTPase activity, could explain the opposed effects of GIMAP4 and GIMAP5 in lymphocyte survival (Cambot et al., 2002; Nitta et al., 2006; Schnell et al., 2006; Schwefel et al., 2013). A similar type of heterodimerization between GIMAP4 and GIMAP5 and subsequent GTP-hydrolysis could disrupt the GIMAP5 scaffold, leading to dissociation from anti-apoptotic factors and eventually, to apoptosis (Nitta et al., 2006; Schwefel et al., 2013; Yano et al., 2014). The hypothesis of heterodimerization was also supported by mRNA microarrays of anaplastic large cell lymphoma cell lines, in which both *GIMAP4* and *GIMAP7* were downregulated whereas *GIMAP2* was expressed in all and *GIMAP5* in half of the cell lines (Poirier et al., 1999; Schwefel et al., 2013).

1.2.3 Autophagy-related protein 5 in adaptive immunity

Autophagy-related protein 5 (Atg5) is a member of the Atg12 conjugation system in autophagy, a ubiquitous degradation pathway of the cell. Atg5 forms a complex with Atg12 that enables the elongation of the membrane to autophagosome vesicle, which is eventually degraded in lysosomes. This complex formation is a prerequisite for autophagy to proceed (Mizushima et al., 2003; for review see Levine and Deretic, 2007).

Autophagy genes are expressed in both human and mouse T lymphocytes and the expression is elevated after activation of the T cell –receptor (Gerland et al., 2004; Pua et al., 2007; Nedjic et al., 2008). Besides producing self-antigens for the positive and negative selection of T lymphocytes (Nedjic et al., 2008; for review see Walsh and Edinger, 2010), autophagy, and especially *Atg5*, is essential for the homeostasis of T cells (Pua et al., 2007; for review see McLeod et al., 2012). *In vivo* studies using lethally irradiated mice repopulated with haemotopoietic cells from fetal livers of *Atg5-/-* mice showed that the proliferation of peripherial $CD4^+$ and $CD8^+$ T cells was inefficient after T-cell receptor stimulation but had no effect on the maturation or differentiation of T cells. This could be explained by the inefficient reduction of mitochondria during the maturation, leading to elevated levels of reactive oxidative species (ROS) and excessive apoptosis of peripheral T cells. Alternatively, a defective autophagy could fail to produce enough nutrients for T cell proliferation (Hildeman et al., 1999; Pua et al., 2007).

Besides providing antigens to present on MHC class II molecules and affecting the MHC-II antigen-processing machinery (Dengjel et al., 2005; Schmid et al., 2007; Kondylis et al., 2013), autophagy is also connected to cross-presentation of antigens to CD8+ T cells by dendritic cells (Li et al., 2009). In addition, the dendritic cell –specific deletion of *Atg5* impaired the CD4+ T cell priming in mice (Lee et al., 2010).

1.3 Inheritance and segregation of mitochondrial DNA

The mitochondrial genome exists in multiple copies, which are organized into nucleoids composed of double-stranded circular DNA strands associated with various proteins (Anderson et al., 1981; Miyakawa et al. 1987; Garrido et al., 2003). These nucleoids are attached to the inner membrane of mitochondria (Satoh and Kuroiwa, 1991). The inheritance pattern of mitochondrial DNA (mtDNA) differs from the pattern of the nuclear genome because mtDNA is inherited maternally, representing cytoplasmic inheritance to which Mendelian genetics do not apply (Dawid and Blackler 1972).

MtDNA molecules can be identical (homoplasmy) or there can be two or more variants (heteroplasmy) in an individual or a cell. Some of these mtDNA variants can be pathogenic and cause inefficient translation and function of respiratory complex proteins leading to decreased production of ATP, affecting especially muscles and nervous system with high demand of energy. Mutations in the nuclear-encoded mitochondrial proteins can also give rise to mitochondrial disorders, because they are essential for the mtDNA maintenance and segregation (for review see Taylor and Turnbull 2005). Pathogenic mtDNA variants in somatic tissues were shown to affect the segregation pattern of mtDNA, which can vary depending on the mutation, cell type and nuclear background. This segregation pattern is noticed to affect the severity and the onset of the disease (for review see Grossman and Shoubridge, 1996; Battersby et al., 2003; DiMauro and Schon, 2003). Understanding the mechanism behind mtDNA segregation could help control the segregation patterns of pathogenic mtDNA mutations that cause mitochondrial disorders in humans (Battersby et al., 2003).

1.3.1 Segregation of mitochondrial DNA under nuclear control

Although the general transmission of heteroplasmic mtDNA variants to daughter cells is thought to be random depending on the mtDNA copy number and turnover rate (Chinnery and Samuels 1999), the segregation phenotype can be altered by the haplotype or tissue, resulting in the selection of one mtDNA haplotype over another (Chinnery et al., 1999;

Weber et al., 1997). The study of two old inbred mouse strains, NZB and BALB/c, possessing two non-pathogenic mtDNA haplotypes showed tissue-specific and age-related directional selection for the NZB variant in liver and kidneys and the BALB variant in hematopoietic tissues (Jenuth et al., 1997). Unlike the NZB genotype, the selection of the BALB genotype is proportional in hematopoietic tissues, which never become fixed with the BALB genotype (Battersby and Shoubridge 2001; Battersby et al., 2005). The segregation pattern was not affected by enhanced OXPHOS capacity or replicative advantage over another genotype (Battersby and Shoubridge 2001). By analyzing the gene linkage study results of the segregation phenotype in F2 intercross of *Mus musculus domesticus* (BALB/c) and the subspecies *Mus musculus castaneus* (CAST/Ei), the first nuclear gene *Gimap3*, was identified to modify the segregation in mammalian hematopoietic tissues. The segregation was tissue-specific but the details of the mechanism involved are still unknown (Jokinen et al., 2010).

1.3.2 Morphological changes of mitochondria influence the maintenance and segregation of mitochondrial DNA

The constant morphological changes of eukaryotic mitochondria from fragmented to elongated through fission and fusion in diverse metabolic conditions (Rossignol et al., 2004; Karbowski et al., 2006) is connected to several cellular processes including maintenance and nonrandom inheritance of mtDNA to daughter cells in *Saccharomyces cerevisiae* (Nunnari et al., 1997; Hanekamp et al., 2002). In human cells, the silencing of mitochondrial fission protein *Drp1* causes defects in mitochondrial fission leading to increased levels of mutant mitochondrial mtDNA compared to wild-type mtDNA (Malena et al., 2009). Therefore, demonstrating that the mitochondrial network is essential in determining the mutant load of mtDNA, and supported earlier findings that the segregation of mutant mtDNA is not always a result of random genetic drift (Dunbar et al., 1995; Holt et al., 1997; Nunnari et al., 1997; Malena et al., 2009).

1.3.2.1 A membrane tethering protein complex affects the maintenance and segregation of mitochondrial DNA

Both in yeast and humans ER tubules wrap around mitochondria indicating the constriction site of mitochondrial division and the assembly-site of ring-like structure of fission protein, dynamin-related proteins Dnm1 in yeast and Drp1 in humans (Bleazard et al. 1999; Smirnova et al. 2001; Friedman et al. 2011; Murley et al., 2013). In yeast, a multiprotein complex called ER-Mitochondria Encounter Structure (ERMES), composed of proteins localized to the ER (Mmm1 and Mdm12) and outer-membrane of mitochondria (Mdm10, Mdm34 and Mdm12), works as a tether in these membrane contact sites. Components of ERMES are also needed to maintain the morphology of mitochondria, the segregation of mitochondria and stability of mtDNA from mother to daughter cell during mitosis but also within the cell (Burgess et al., 1994; Sogo and Yaffe, 1994; Berger et al., 1997; Nunnari et al., 1997; Boldogh et al. 1998; Hobbs et al., 2001; Hanekamp et al., 2002; Kornmann et al., 2009; Murley et al., 2013). Defects in these proteins lead to the collapse of mitochondrial morphology from tubular to spherical form, which has been related to instability and loss of mtDNA as well as defects in inheritance of mtDNA to daughter cells (Burgess et al., 1994; Hobbs et al., 2001; Hanekamp et al., 2002; Boldogh et al., 1998). These findings are supported by the localization of ERMES and its components next to the segregating and actively replicating mtDNA nucleoids (Hobbs et al., 2001; Murley et al., 2013; Meeusen and Nunnari, 2003). In humans, the nucleoids also localize to mitochondrial division sites (Garrido et al., 2003; Iborra et al., 2004).

Similar complexes are believed to exist in other eukaryotic cells as well, because Mmm1 and Mdm12 belong to the synaptotagmin-like-mitochondrial-lipid binding protein (SMP)-domain protein family, which has multiple members across eukaryotic cells, humans to plants (Lee and Hong, 2006). SPM-domain was shown to be necessary for targeting proteins to membrane contact sites, such as the ER-mitochondria and ER-plasma membrane (Toulmay and Prinz, 2012).

2 AIM OF THE STUDY

With exception of Bcl-2 family members, little is known about proteins interacting with Gimap3. The discovery of new interacting proteins would clarify the mechanisms by which Gimap3 functions in the cell and in particular, its role in the segregation of mtDNA. Preliminary genetic studies by the Battersby group suggested that the stability of Gimap3 was dependent on the expression of functional Atg5. Whether these two proteins interacted directly or not was so far unknown.

The goal of this study was to optimize a co-immunoprecipitation (co-IP) protocol for studying the protein interactions of Gimap3 and also, to find out whether Atg5 interacts with Gimap3. The focus was to set up an optimized co-IP protocol with good recovery of Gimap3 and minimal background contaminants. This required finding a good and reliable antibody to precipitate Gimap3, but also an optimal detergent for Gimap3, and salt concentration of wash buffers and enrichment method of bait protein to decrease the background.

3 MATERIALS AND METHODS

3.1 Retroviral expression and cell culture

Full-length cDNAs (BALB *Gimap3*, BALB *Gimap3-HA, GFP-(261-301) Gimap3*) were cloned into Gateway (Invitrogen) converted retroviral expression vectors: pBABE-puro, pMYS-IRES-Neo, or pMX-IRES-Blasticidin. These retroviral vectors were transfected (Jetprime, Polyplus) into the Phoenix amphotropic packaging line for virus production to infect recipient cells: wild-type mouse embryonic fibroblasts (MEFs), human embryonic kidney cell line (HEK293) or mouse lymphoblasts (EL4). Cells were selected on the appropriate antibiotics before being used in experiments. Dr. Brendan Battersby and laboratory technician Paula Marttinen established all the cell lines.

Cells were cultured in standard conditions in DMEM (Euroclone/Lonza) with 10% fetal bovine serum (GIBCO®) and 4,5g/l glucose at +37°C, 5% CO_2 in aerobic conditions. Cells were passaged to 1:5 twice a week by detaching the cells with 10x trypsin (GIBCO®) at +37°C. The confluency of EL4 cells was determined by Countess Automated Cell Counter (LifeTechnologies™) and cells were collected in full confluence by Dr. Brendan Battersby. Other cells were collected at 80-90 % confluence either by scrapping or trypzinisation into ice-cold 1xPBS. Cell pellets were washed once with ice-cold 1xPBS. All the cells were pelleted at 10 000 xg or 18 000 xg (Beckman Coulter™ – Allegra™ X-22R Centrifuge) from 30 seconds to two minutes at +4°C. Pellets were stored at -80°C.

3.2 Homogenization and differential centrifugation

Teflon-dounce homogenizer was used for disrupting the cells resuspended in HIM buffer (App. 2). Starting material 1 (SM-1) sample was collected from the homogenized cell lysate and lysed. Differential centrifugation (DC) followed homogenization. In DC I, the nucleus and organelles not disrupted by homogenization, were separated from the cytoplasmic material (Fig. 3, A). The nuclear pellet (NP) was collected. In the next centrifugation (Fig. 3, B) all the intracellular membrane structures (heavy membrane

pellet=HMP), such as mitochondria and parts of ER, were separated from the soluble cytoplasmic material and vesicles (light membrane pellet=LMP). HMP was resuspended into 1 ml of HIM buffer and pelleted using the same settings as in step B. HMP was used for co-IP experiments.

DC II protocol (Fig. 3) differed from DC I in that the NP pellet was washed four times with 30 ml HIM buffer per wash (Fig. 3, C). Centrifugation was repeated after every wash (Fig. 3, red arrows). The last pellet was collected as NP sample. All the four supernatants from the washes were centrifuged as in step B and the pellets were resuspended into HIM buffer and combined to 30 ml of HIM buffer (Fig. 3, D). Centrifugation was repeated and the supernatant was collected as LMP sample and the pellet as HMP sample. Both DC I and II protocols were performed at +4°C using Allegra™ X-22R Centrifuge of Beckman Coulter™ and the LMP sample was concentrated into 1 ml using the concentration tube Amicon Ultra-15 centifugal filter device with filter pore size 3000 MWCO (Millipore).

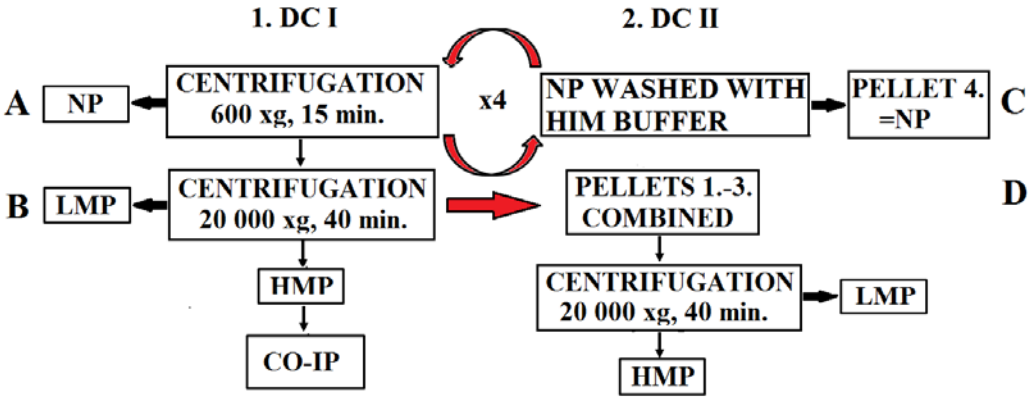

Figure 2: Differential centrifugation I (DC I: left side) and differential centrifugation II (DC II: right side) protocols and the samples collected. NP= nuclear pellet, LMP= light membrane pellet, HMP= heavy membrane pellet, co-IP= co-immunoprecipitation.

3.3 Co-immunoprecipitation

The total protein extract for co-immunoprecipitation (co-IP) was extracted from whole cell or HMP pellet with lysis buffer (App. 2, lysis buffer I and II). After 30 minute incubation on ice, the supernatant was separated from the membrane debris by centrifugation (20 000 xg, 20 min, +4°C). When proteins were extracted from whole cell pellets, some

supernatant (20-30 µl) was left on top of the pellet to prevent nuclear protein contaminations. Protein concentration was measured by Bradford protein assay (Biorad) using Spectra-max 190 (Molecular devices). Starting material 2 (SM-2) was collected from the supernatant.

Protein extract from the lysis (1 µg/µl and 4 µg/µl in crosslinking co-IPs) was first incubated with 5 or 10 µg of antibody. Mouse monoclonal anti-HA antibody (1,2 µg/µl; Clone HA-7 Purified Mouse Immunoglobulin; Sigma-Aldrich) was used for the precipitation of recombinant Gimap3 with N-terminal human influenza hemagglutinin (HA) tag and purified mouse IgG antibody (1,0 µg/µl; Purified Immunoglobulin; Sigma-Aldrich) as the control antibody. Next, this protein extract was incubated with 1:2 G-sepharose bead slurry (Protein G Sepharose™ 4 Fast Flow (GE Healthcare)). The green fluorescent protein (GFP)-tagged transmembrane domain (261-301) of Gimap3 (GFP-(261-301)Gimap3) was precipitated with 10 µl of Chromotek-GFP-Trap® (Chromotek) magnetic beads. Altogether incubations lasted 2 hours on a rotator. Flow-through (FT) was removed by centrifugation (12 000 xg, 30 sec.) and unbound proteins were removed by washing four times with 1,2 ml wash buffer. Wash samples were collected as well as FT. Either all four washes (W- 1-4) had low salt concentration (140-150 mM) or the first three washes were with high salt concentration (400 mM) followed by one low salt concentration wash (App. 2, wash buffer I and II). Proteins were eluted in 1x Laemmli loading buffer (App. 2) by incubating the beads at +95°C- +100°C. The whole protocol was performed at +4°C using Allegra™ X-22R Centrifuge (Beckman Coulter™) for all the centrifugations.

3.4 Trichloroacetic acid-precipitation

Proteins were precipitated by adding trichloroacetic acid (TCA) to a final concentration of 13% and pelleted by centrifugation at 20 000 xg for 30 minutes. Lipids and residual TCA were removed by washing the pellet twice with ice-cold 100% acetone. Acetone was removed by centrifugation at 20 000 xg for 5 minutes. After the pellet was air-dried, it was resuspended in 1xLaemmli loading buffer (App. 2) into the same volume as the co-IP

elution. The pH of the sample was adjusted with 2M NaOH if the sample was too acid and turned yellow. The last sample was heated at +95°C or +100°C for 5-10 minutes. All the centrifugations were performed in Allegra™ X-22R Centrifuge of Beckman Coulter™.

3.5 Immunoblotting and silverstaining

Proteins were separated in 10 or 12% SDS-PAGE gel (sodium dodecyl sulfate polyacrylamide gel) in 1x TG-SDS buffer (App. 2) using the Mini-PROTEAN® 3 Tetra Cell (Bio-Rad). PageRuler Prestained protein ladder 10-70 K (Fermentas) was used as a protein size marker. Samples in the SDS-PAGE gel were transferred to Hybond™-ECL nitrocellulose membrane (Amersham) in semidry transfer buffer (App. 2). A successful transfer and equal loading were ensured by dying the membrane with reversible Ponceau S Solution (Fluka). The unspecific binding of antibodies was prevented by blocking the membrane with either 5 % bovine serum albumin (BSA) or 1,5% Milk (Valio) in +1xTBS-T–solution (App. 2). Primary antibodies (App. 1) were incubated overnight at +4°C and secondary antibodies (App. 1) in 1xTBS-T for one hour at room temperature. Unbound antibodies, both primary and secondary, were washed three times with 1xTBS-T (20 min/wash). Proteins of interest were detected by enhanced chemiluminescence using reagents 20X LumiGLO® Reagent and 20X Peroxide (Cell Signaling Technology®). SuperSignal® Westo Femto Maximum Sensitivity Substrate (ThermoScientific) was used for weaker antibodies. The membrane was exposed to medical X-ray film (Fuji), which was developed in Medical X-ray Processor (KODAK). Some membranes were developed with Immun-Star™ WesternC™ Kit (BIO-RAD) ECL using ChemiDoc™ XRS+ System (Bio-Rad).

Silverstaining of SDS-PAGE gel was performed with SilverSNAP® Stain Kit II (PIERCE) according to the protocol. The buffers for sensitizing, staining and development were provided by the kit. The fix, wash and stop solutions were self-made (App. 2). The development time of the gels was 1 to 2 minutes.

3.6 Mass spectrometry analysis

Tuula Nyman performed the liquid chromatography-electrospray ionization tandem mass spectrometry (LC-MS/MS) analysis in Biocenter 3, using an Ultimate 3000 nano-LC (Dionex) and a QSTAR Elite hybrid quadrupole TOF-MS (Applied Biosystems/MDS Sciex) with nano-ESI ionization. Proteins were cleaved by trypsin prior to analysis. For the protein identification database searches were performed using Mascot search engine (Matrix Science, London, UK) with a tolerance of ± 50 ppm for peptide mass and ± 0.2 Da for the fragment mass against SwissProt 2011 database (531473 sequences; 188463640 residues). The significance threshold was $p<0,05$. One missed cleavage site was accepted for trypsin, carbamidomethyl cysteine modification was considered as fixed modification and methionine oxidation, phosphorylation of serine, threonine and tyrosines as variable modifications. Mass value parameter was chosen as monoisotopic and protein mass was unrestricted.

3.7 Crosslinking experiments

Crosslinking was performed for the HMP or whole cell pellet resuspended into HIM buffer by adding 1,2 µl of 30 mM crosslinker in anhydrous DMSO. Anhydrous DMSO by itself was used as negative control. Crosslinking reaction was quenched with excess of amines using 0,5 M glycine suspension (App. 2) at different timepoints (20, 40, 60, 180 minutes). Samples were centrifuged at 20 000 xg for 40 minutes and the pellet was washed with HIM buffer to discard the remaining crosslinker reagent. Lysis was performed with the same lysis buffer used in co-IP and 1x 1xLaemmli without β-mercaptoethanol was added 1:1 into the supernatant. Except when crosslink of DSP was broken, β-mercaptoethanol was added to a final concentration of 5% (v/v). Incubation lasted 10 minutes at +55°C, except when the crosslink was broken down and the samples were incubated at +100°C.

4 RESULTS

4.1 Anti-HA antibody precipitated the bait protein specifically and efficiently

The affinity and specificity of anti-HA antibody, as well as the optimal amount of antibody for efficient precipitation, were detemined performing precipitation experiments with 5 and 10 µg of antibody for whole cell pellet protein extracts. Because a commercial antibody highly specific against BALB Gimap3 was not available, an anti-HA antibody against HA-tagged Gimap3 (from now on referred as Gimap3) was used. The 5 µg of anti-HA antibody precipitated Gimap3 more efficiently than the double amount of antibody. As Gimap3 was not detected in the elution of the control co-IP using mouse IgG antibody, the specificity of the anti-HA antibody to Gimap3 was also confirmed (Fig. 4 A). These results were further confirmed by repeating the co-IP assay using the same protocol with 5 µg of anti-HA antibody (Fig. 4 B). However the amount of precipitated Gimap3 (34 kDA) was under detectable levels in the silverstained gel (Fig. 4, B). The heavy (55 kDA) and light (25 kDA) chains of antibody dominated the staining results (Fig. 4 B).

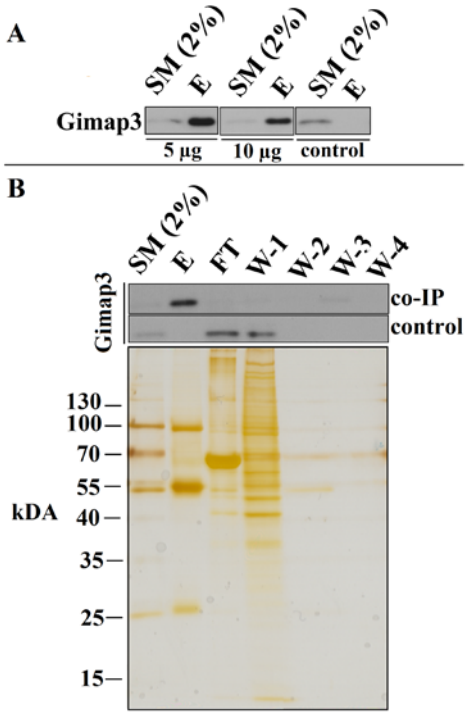

Figure 3: Specificity and precipitation efficiency of anti-HA antibody: (A) Detection of Gimap3 in immunoblots. Anti-HA antibody precipitated Gimap3 efficiently and specifically and the recovery of Gimap3 in the elution (E) was greater with 5 µg than 10 µg of antibody. The control co-IP confirmed specific precipitation of Gimap3, which was not detected in the control elution. Immunoblots were exposed at the same time. **(B) Gimap3 antibody detection and corresponding SDS-PAGE analysis by silverstaining.** Repeating the co-IP with the optimal amount of 5 µg of anti-HA antibody confirmed the results of antibody optimization as shown by Gimap3 antibody detection. However the level of precipitated Gimap3, which runs around 34 kDA, was undetectable after staining the gel with highly sensitive silverstaining for 40 seconds. Samples were equally loaded in each experiment (A and B).

4.2 Enrichment of bait protein by differential centrifugation

Due to undetectable levels of Gimap3 in elution by silverstaining, Gimap3 was enriched by differential centrifugation (DC). At the same time, DC was expected to reduce background contaminations in the eluted samples. In DC I, a greater amount of Gimap3 was detected in the NP sample than in the HMP one. However, it is noteworthy that due to accidental unequal loading of the samples, the NP lane contains more protein than in reality (Fig. 5, DC I). Still, the recovery of Gimap3 in the HMP fraction was good compared to the SM-1 sample (Fig. 5, DC I). Compartmental markers for ER (Calnexin), mitochondria (Tom40) and cytoplasm (Cops5) were found in NP samples, indicating the incomplete separation of cell compartments (Fig. 5, DC I). Tom40 and Calnexin were detected in HMP sample as well (Fig. 5, DC I).

In order to increase the amount of Gimap3 in the HMP fraction, the NP pellet was washed with HIM buffer in DC II. However, the recovery of Gimap3 in the HMP fraction was not improved. Although Gimap3 was no longer detected in the NP sample, the amount of Gimap3 in HMP was significantly smaller than in the SM sample (Fig. 5, DC II).

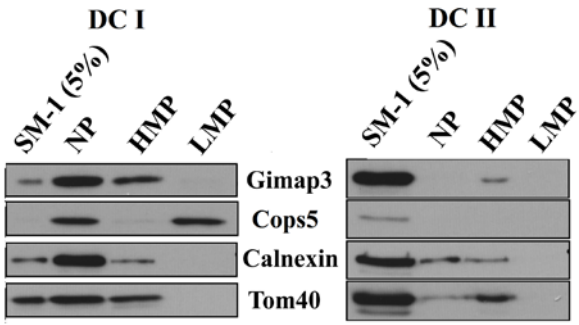

Figure 5: Enrichment of Gimap3 by DC. Due to incomplete separation of cell compartments, as indicated by three distinct compartmental markers (Cops5=cytoplasm, Calnexin=ER, and Tom40=mitochondria), some Gimap3 was lost to the NP pellet. However as highlighted in the main text, the uneven loading of samples resulted in a higher concentration of Gimap3 in the NP fraction. Some Calnexin and Tom40 were detected in the HMP samples. In DC II, the washing of the NP pellet did not increase the recovery of Gimap3 to the HMP pellet. Instead, most of Gimap3 and compartmental markers were detected in the SM sample. Percentage of TCA-precipitated sample volumes loaded in to the gel in DC I: SM and NP (100%), HMP and LMP (35%). DC II: 100% of all sample volumes was loaded. SM-1= starting material, NP= nuclear pellet, HMP=heavy membrane pellet and LMP= light membrane pellet.

4.3 The balance between good recovery of bait protein and the amount of background contaminations in the elution was optimal with n-dodecyl β-D-maltoside

Different detergents combined with low and high salt concentration washes were tested to find an optimal detergent solubilizing Gimap3 and providing high recovery of bait protein in the elution. The recovery of Gimap3 in elution from the SM samples was reasonably high with both *n*-dodecyl β-D-maltoside (DDM) and sodium taurodeoxycholate hydrate (STDC) combined with low salt concentration washes (LOW) (Fig. 6 A). When combined with high salt concentration washes (HIGH), the recovery of Gimap3 remained high in the elution fraction with STDC (Fig. 6 A). Also, similar recovery levels were detected using octyl-β-D-glucopyranoside (OGP) (Fig. 6 A). In contrast, the recovery was extremely low with digitonin (DG) (Fig. 6 A). No significant contamination levels from other cell compartments or Gimap3 were detected in any of the control co-IP elutions (Fig. 6 A).

Some Gimap3 was always lost to the flow-through (Fig. 6 A and B), but fortunately comparison between flow-through and low and high wash samples of STDC showed no greater loss of Gimap3 to the high salt concentration washes (Fig. 6 B).

However, the silverstaining of the gel-fragmented elutions showed high levels of background when DDM and STDC combined with low salt concentration washes were used (Fig. 6 C). There was some background as well in the elutions with STDC, OGP and DG combined with high salt concentration washes (Fig. 6 C). The level of background between low and high salt concentrations cannot be compared because the gels were developed in separate experiments.

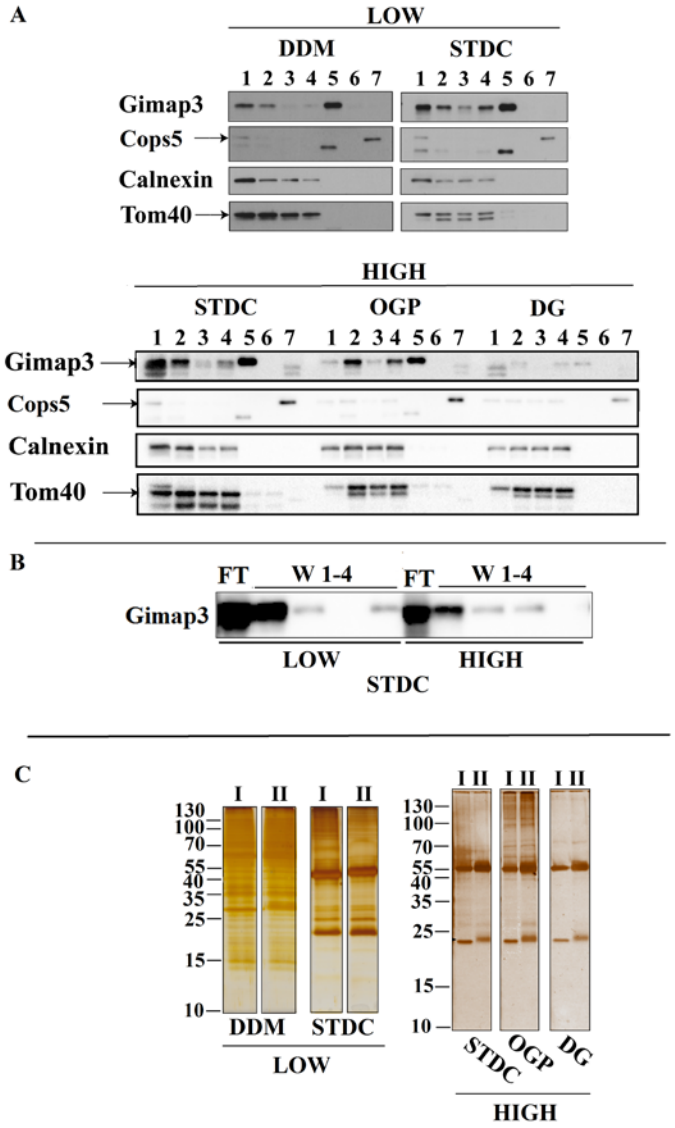

Figure 6: (A) The recovery of Gimap3 in the elutions using different detergents combined with low and high salt concentration washes: antibody detection of Gimap3. The recovery of Gimap3 is shown using different detergents in low and high salt concentration conditions. Recovery was substantial with all detergents, except digitonin (DG). Cops5, Calnexin and Tom40 were used as markers to verify proper cell compartment separation by DC. Gimap3 was not detected in control co-IP elutions. **(B) Loss of Gimap3 to FT and W samples in low and high salt conditions.** Similar amounts of Gimap3 were lost to the flow-through and wash samples of STDC when high and low salt concentration washes were used. **(C) Levels of background contaminations in the elutions.** The background of elutions with DDM and STDC combined with low salt concentration washes (LOW) was high. Some background was also detected with STDC, OGP and DG using high salt concentration washes (HIGH). Concentrated Gimap3 (34 kDA) was not detected in any of the elutions. The intense bands of heavy (55 kDA) and light (25-26 kDA) chains of both antibodies dominated the staining results. Background levels between the co-IP and control co-IP elutions did not differ significantly, which could be caused by unspecific binding of proteins to the beads. I= the elution with anti-HA, II= control elution with IgG. Gels with low and high salt concentration washes were developed separately but the development time was 1 minute for all the gels. Protein concentration of samples loaded: 20 µg (DDM LOW, STDC and OGP HIGH), 28 µg (STDC LOW), 15 µg (DG HIGH). 1= SM-1, 2= SM-2, 3=FT (anti-HA), 4= FT (control), 5= E (anti-HA), 6=E (control), 7=LMP.

4.3.1 Increasing the recovery of bait protein in the elution

The recovery of Gimap3 in the elution was tried to increase by repeating the co-IP for the flow-through using STDC and high salt concentration washes Although Gimap3 was not detected in the flow-through of the second co-IP, the recovery of Gimap3 in the second elution was not significantly improved (Fig. 7).

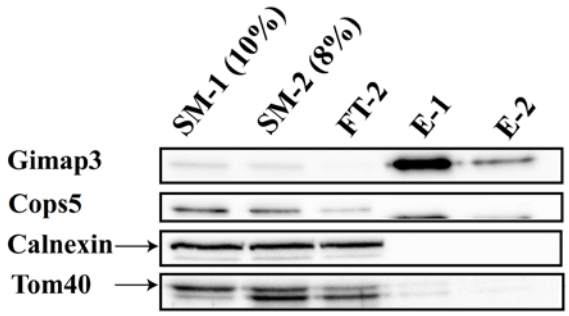

Figure 7: Co-IP of flow-through of first co-IP. An attempt to recover Gimap3 from FT was made by running a second co-IP for the FT using STDC and high salt concentration washes. Although Gimap3 was hardly detected in the flow-through of the second co-IP (FT-2), the recovery of Gimap3 was not increased significantly (E-2). Samples were equally loaded. SM-1= starting material-1, SM-2= starting material 2, FT-2=flow-through of second co-IP, E-1= elution of first co-IP, E-2= elution of second co-IP.

4.4 Identification of interacting proteins by mass spectrometry

Gimap3 was successfully precipitated from protein extracts from T cells, where it is normally expressed. However, silverstaining revealed the background of elution to be too high for performing reliable mass spectrometry analysis (Fig. 8 A and B). Gimap3 was not detected in any other sample than the elution, Cops5 was found in none of the samples (Fig. 8 A). The co-IP performed on the green fluorescent protein (GFP)-tagged transmembrane domain (261-301) of Gimap3 (GFP-(261-301)Gimap3) using magnetic beads had low levels of background in the elution (Fig. 8 B). Unfortunately, due to the lack of a specific anti-GFP antibody, immunoblot detection and verification of precipitation efficiency were not possible. But the intense band in the elution running below 35 kDA marker (shown by an arrow) was compatible with the size of GFP-(261-301)Gimap3 (~ 31 kDA) and gave confidence to continue to mass spectrometry analysis (Fig. 8 B). The only

chain of antibody, attached to the magnetic beads, with a size of 13 kDA (Chromotek) was detected in the lower part of the gel (Fig. 8 B).

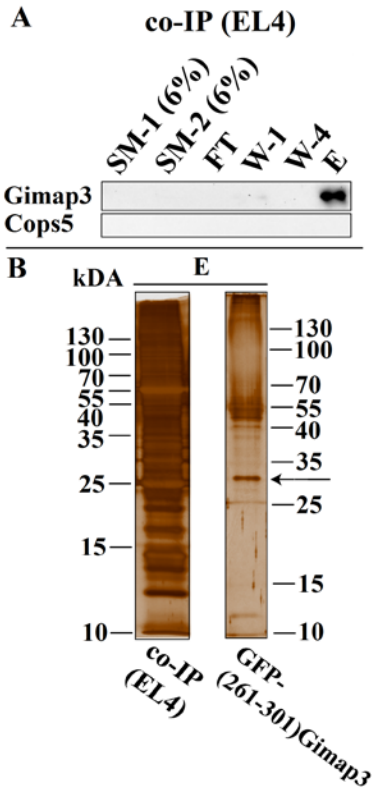

Figure 8: (A) Co-IP experiment of Gimap3 extracted from lymphoblasts. The precipitation of Gimap3 from T cells (EL4) with STDC and high salt washes was successful, although Gimap3 was not detected in any other sample except the elution. Cops5 was not detected in any sample. Equal volumes of TCA-precipitated samples were loaded. **(B) Silverstained SDS-PAGE of the elution samples indicating background levels.** Besides contaminations from the heavy (55 kDA) and light (25-26 kDA) chains of antibody, background levels in the elution of co-IP performed against Gimap3, extracted from T cells, was extremely high. In contrast, it was low in the elution of GFP-(261-301)Gimap3 using DDM and high salt concentration washes. The intense band in the elution (indicated by an arrow) matches the size of the bait protein (31 kDA). The antibody chain of 13 kDA ran below the 15 kDA size marker. Both gels were developed for two minutes.

4.4.1 Identified interaction partners

The threshold score being 41, a total number of 69 proteins were identified from the elution of GFP-(261-301)Gimap3. 41 of these proteins were not detected in the control elution with mouse IgG, suggesting potential interactions with transmembrane domain of Gimap3. Only one prospective and interesting protein interaction partner, vesicle trafficking protein SEC22b (SEC22b) (Q4KM74|SC22B_RAT) with score 45, was found

in the mass spectrometry analysis. Because Gimap3 has been suggested to localize to the ER, the localization of SEC22b to ER-Golgi intermediate compartment made it a putative interaction candidate (Cebrian et al., 2011). The transmembrane domain of Gimap3 was not detected but the GFP-tag was with score 107 (App. 3). No evidence supporting protein interactions between Atg5 and Gimap3 was discovered (App. 3). Most likely due to the sample handling, elution was also highly contaminated with keratin which dominated the results with the highest score (App. 3).

4.5 The crosslinking of the bait protein

Preliminary crosslinking experiments were performed to allow more stringent washes in order to bring down levels of background contaminants. Both 1,5-difluoro-2,4-dinitrobenzene (DFDNB) and disuccinimidyl glutarate (DSG) were extremely efficient crosslinkers, because Gimap3 was either immediately undetectable (DFDNB) or was hardly noticeable after 20 minutes of incubation (DSG) (Fig. 9). Efficiency of crosslinkage with disuccinimidyl suberate (DSS) and dithiobis[succinimidylpropionate] (DSP) increased in linear fashion with the incubation time (Fig. 9). Efficiency was determined by comparing the amount of detected Gimap3 at different timepoints with a negative control. Shifted bands of Gimap3 (>130 kDA), potential crosslinked protein complexes, were detected only with DFDNB and DSP (Fig. 9). DFDNB was the only crosslinker reacting with Atg5 and Tom40 (Fig. 9). None of the crosslinkers were able to crosslink Calnexin (Fig. 9). As a thiol-cleavable crosslinker, the crosslink of DSP was only reversible one and successfully broken down with β-mercaptoethanol, which disrupts the sulphur bridges (Fig. 9). Shifted bands disappeared and Gimap3 was detected around the excepted 34 kDA (Fig. 9).

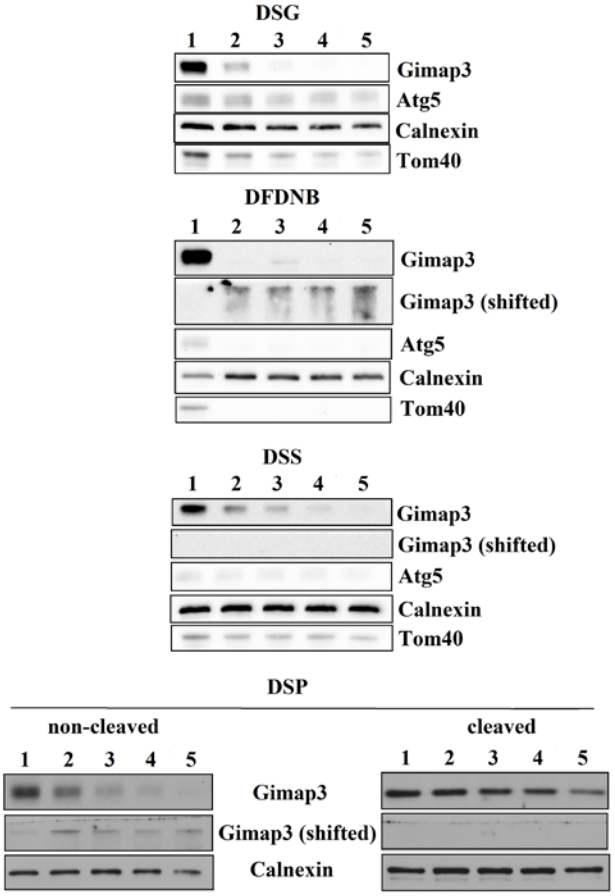

Figure 9: Crosslink experiments. All crosslinkers crosslinked Gimap3 successfully and that was indicated by a faint to absent band around 34 kDA. DFDNB was the most efficient crosslinker and Gimap3 was immediately undetectable (lane 2). With DSG, Gimap3 was undetectable after 20 minutes (lanes 2-3). With DSS and DSP, the crosslinking efficiency correlated with incubation time (lanes 2-5). Shifted bands, running above the 130 kDA size marker, appeared only when DFDNB and DSP were used. As a thiolcleavable crosslinker, the crosslinkage of DSP was reversible. This was indicated by the disappearing of shifted bands of Gimap3 and detection of Gimap3 as a neat band around 34 kDA. Equal volumes were loaded into gels. 1= negative control (no crosslinker), 2= 20 minutes, 3= 40 minutes, 4= 80 minutes and 5=180 minutes incubation time.

4.5.1 Co-immunoprecipitation of crosslinked bait protein was unsuccessful

Precipitation of DSP-crosslinked Gimap3 was unsuccessful when both HMP and whole cell pellets were used as starting material and STDC as detergent combined with high salt concentration washes (Fig. 10). Except for the flow-through (FT) and first wash sample (W-1) of co-IP with HMP, Gimap3 was not detected in the immunoblot, even though the

crosslinkage was broken down by β-mercaptoethanol. Gimap3 was also undetectable in both control co-IPs (Fig. 10).

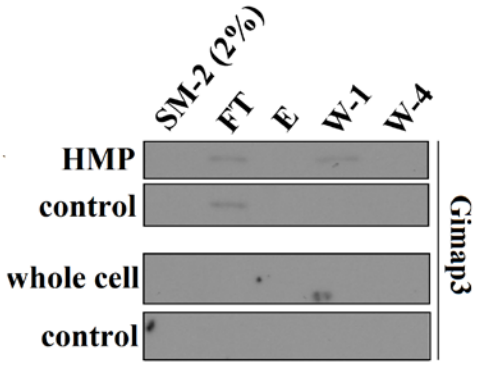

Figure 10: Co-IP of DSP-crosslinked Gimap3. With both HMP and whole cell pellets as starting material the precipitation of DSP-crosslinked Gimap3 was unsuccesful. Some Gimap3 was detected in the FT and in the first wash (W-1) of HMP co-IP, but in any other samples including control co-IPs, Gimap3 was undetectable despite the crosslinkage being broken down with β-mercaptoethanol. SM sample was collected before the co-IP protocol: SM-2= starting material-2, FT= flow-through, E= elution, W-1= wash sample 1, W-4= wash sample 4.

5 DISCUSSION

5.1 Optimization of co-immunoprecipitation

5.1.1 Determining the antibody specificity and precipitation efficiency

Gimap3 is known to modify the segregation of mtDNA, but also to take part in T cell maturation and maintenance of their homeostasis with Gimap5 and members of the Bcl-2 family (Nitta et al., 2006; Dalberg et al., 2007; Jokinen et al., 2010; Yano et al. 2014). However, the mechanisms behind these cellular processes and how Gimap3 works in these events are still unknown, especially in mtDNA segregation. Therefore, the aim of this study was to identify proteins interacting with Gimap3 using co-IP as the main method. Protein interactions are studied by co-IP of the protein of interest, known as the bait protein, and the proteins interacting with it, the prey proteins, using an antibody highly specific to the bait protein (for review see Hall, 2005; for review see Berggård et al, 2007). Usually, monoclonal antibodies are preferred because of their specific binding to the bait protein. Polyclonal antibodies could eventually interact with other proteins in a non-specific way (for review see Phizicky and Fields, 1995). The bait-prey-antibody protein complex is stabilized on a matrix, for example G-sepharose beads, which is washed to eliminate the non-specifically binding proteins, the background. The eluted proteins are then analyzed by immunoblotting and mass-spectrometry (for review see Hall, 2005; for review see Berggård et al, 2007).

Because no highly specific monoclonal antibody against BALB Gimap3 was available, the commercial monoclonal anti-HA antibody was used to precipitate recombinant Gimap3 with a N-terminal HA-tag (for review see Hall, 2005). As a small tag, HA was less likely to interfere with the folding and structure of Gimap3 (Bucher et al., 2002). Although Gimap3 was precipitated efficiently, this did not confirm whether Gimap3 had kept its native conformation, which could affect its function and interactions with other proteins. The specificity for Gimap3 and precipitation efficiency of anti-HA antibody were confirmed by comparing the recovery of Gimap3 in the elution to the amount of Gimap3 in the starting material by immunoblotting as well as running a control co-IP in parallel (Fig.

4 A) (for review see Hall, 2005). As one would expect, no bait protein should be detected in the control elution. Steric hindrance caused by a high amount of antibodies competing for the same epitope, might explain the lower recovery of Gimap3 in the elution when using the double amount of anti-HA antibody (Metz et al., 2012), leaving 5 µg of anti-HA antibody the optimal amount of antibody. Because the mouse IgG is from the same organism as the bait protein, it was not expected to interact with proteins from the same organism and therefore, was considered to be a safe choice to use as control antibody.

False positive interactions could be formed during disruption of cell and membrane compartments, when proteins accumulate and form false positive protein interactions not occurring *in vivo* (for review see Berggård et al., 2007). False positives as a result of unspecific binding of the antibody were reduced by detecting the bait protein with a different antibody in immunoblotting, anti-BALB Gimap3. Also, false positives were limited by excluding the protein bands appearing in the elutions of both co-IP and control co-IP generated by unspecific binding of proteins to the beads for example (for review see Hall, 2005; for review see Berggård et al, 2007).

5.1.2 An optimal detergent with good protein solubilization efficiency

As each protein and detergent has different chemical properties and some lipids and proteins can hinder the micelle formation of detergents, finding an optimal detergent can only be accomplished through trial and error (for review see le Maire et al., 2000). By nature, detergents are amphipathic as their structure is formed of polar and occasionally charged head groups, and hydrophobic hydrocarbon or steroidal tails (Fig. 11). The use of ionic detergents, with cationic or anionic head groups, in co-IPs is contradictory because they have tendency to denature the protein or break interactions between interacting proteins. They are also incompatible with mass spectrometry analysis (for review see le Maire et al., 2000; for review see Seddon et al., 2004). By lacking charged head group, non-ionic detergents, on the other hand, break interactions between lipids and proteins leaving protein-protein interactions intact. Also, their non-denaturating properties preserve the biological activity of proteins (for review see Seddon et al., 2004). These were the

reasons, why DDM was chosen over ionic sodiumtauro deoxycholate, which solubilized Gimap3 well but was incompatible with tandem mass spectrometry. Zwitterionic detergents, able to change their charge and therefore, having properties of both ionic and non-ionic detergents, were not tested. Besides the charge, detergents also differ in micelle size (for review see Garavito and Ferguson-Miller, 2001; for review see Seddon et al., 2004).

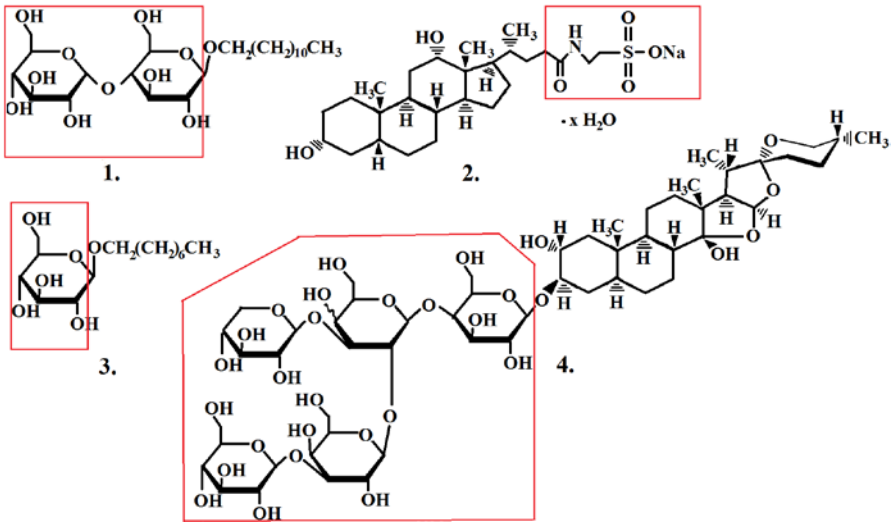

Figure 11: Chemical structures of detergents. DDM (1.), octyl glucoside (3.) and digitonin (4.) are non-ionic detergents and their polar head groups (red boxes) have no charge. The polarity of the head group (red box) is determined by the number of hydroxyl groups that define the solubility of the molecule to water. Instead of polar head group, sodium taurodeoxyhcholate (2.) has anionic one. The hydrophobic tail interacts with the hydrophobic parts of proteins, although the tail of sodium taurodeoxycholate and digitonin is steroidal and the hydroxyl groups make the tail slightly polar.

As a membrane protein, Gimap3 is not water-soluble and its solubility will depend on the chemical properties of the detergent. The better solubility, in turn, increases the amount of precipitated Gimap3. The solubilization ability of detergents is based on mimicking the natural lipid bilayer of the cell where the membrane proteins reside. Like the tail of phospholipids in the membrane, the hydrophobic tail of detergents interacts with the hydrophobic part of proteins via hydrophobic interactions, when the polar and hydrophilic part of detergent form hydrogen bonds and eletrostatic interactions with the aqueous solution (for review see Seddon et al., 2004).

Critical micelle concentration (CMC) determines the detergent concentration needed for the formation of micelles and successful solubilization (Kragh-Hansen et al., 1998; for

review see Garavito and Ferguson-Miller, 2001). Micelle formation and solubilization occurs in three stages with detergent monomers inserting the membrane bilayer and micelle formation proceeding in tandem with increasing CMC (Kragh-Hansen et al., 1998). To accomplish efficient solubilization, excess amounts of detergent are used, the working concentration varying from 0,5% to 2,0%, as was done in the experiments of this thesis (Tab. 1) (Banerjee et al., 1995). Therefore, CMC should not have been a restricting factor for successful solubilization.

Table 1: Chemical and physical characters of detergents. The temperature in CMC paragraph indicates the temperature at which the CMC was determined by the manufacturer

DETERGENT	CMC (20-25°C)	CMC: LYSIS BUFFER	CMC: WASH BUFFER	MICELLAR MOLECULAR WEIGHT
DDM	0,15 mM	19,6 mM	2,0 mM	50,000
Sodium taurodeoxycholate	1-4 mM	19,2 mM	1,9 mM	3100
Octylglucoside	20-25 mM	34,2 mM	3,4 mM	25,000
Digitonin	<0,5 mM	8,1 mM	0,8 mM	70,000

Accurate determination of optimal CMC is difficult and the experimental and environmental conditions can cause significant fluctuations in the CMC value and efficiency of solubilization (for review see le Maire et al., 2000). With ionic detergents, such as sodium taurodeoxycholate, increasing the salt concentration in buffers brings up the number of counter-ions, which decrease the repulsion between the head groups of detergents with same charge. As a result, CMC is reduced as micelle size is increases, improving the solubilization. Furthermore, increasing the temperature converts the detergent from the crystalline, insoluble form to dissolved monomer until CMC is reached. This critical micellar temperature (CMT) is the lowest temperature at which micelles can form. Performing all the experiments at +4°C might have hindered the micelle formation of detergents and therefore, decreased the solubilization of proteins leading to decreased recovery of Gimap3 in the elution. The longer hydrocarbon tail decreases CMC because of the increased number of formed double bonds and branch points, and therefore can compensate the restrictions of low temperature for the micelle formation. For this reason, DDM with its longer hydrocarbon tail was chosen over the other non-ionic detergent octyl glucoside (Fig. 11), although the background in elution with DDM was higher (for review

see Seddon et al., 2004). Digitonin was excluded due to its low ability to solubilize Gimap3.

5.1.3 Reduction of background in the elution

The high level of background produced by unspecific binding of proteins in one-tag purification method, such as co-IP, was partially decreased with high salt concentration washes and by enrichment of Gimap3 with DC (for review Berggård et al., 2007). Nevertheless, the high abundance of contaminating proteins, such as keratin, interefered with the mass spectrometry analysis and distorted the scores and level of significance. Probably, they also prevented the identification of real interacting protein partners with low expression levels and weak signals making these proteins harder to identify (McCormack et al., 1997; Schirle et al., 2003; for review see Gatto et al., 2010). Fortunately the high salt concentration washes did not significantly decrease the recovery of Gimap3 in the elution.

As the control compartment markers (mitochondria, ER and cytoplasm) pointed out, the drawback of DC was the defective separation of cell compartments due to their similar sedimentation velocities and incomplete disruption of cells by homogenization. Therefore, the success of DC must be always confirmed. Although a fairly efficient reduction of contaminating proteins from other cell compartments, such as nucleus and cytoplasm, was achieved, the incomplete separation led also to insufficient enrichment of Gimap3 further decreasing the signal-to-noise ratio of bait protein (Ou et al., 1995; Hill et al., 1998; Tomoda et al., 2002; for review see Lee et al., 2010). Neither washing the NP pellet nor performing co-IP on the flow-through sample increased the recovery of Gimap3. Gimap3 interactions with proteins in different membrane compartments, such as ER and mitochondria, might have broken down during disruption of membrane compartments in DC leading to the loss of interacting partners (Mannella et al., 1998; Daheron et al., 2001; Friedman et al. 2011; Murley et al., 2013).

The crosslinking of Gimap3 was tested to further reduce background by using even more stringent washes without decreasing the signal of Gimap3 or losing interacting proteins with weak and transient protein interactions (de Gunzburg et al., 1989; for review see Hall, 2005). Although Gimap3 crosslinking was successful, the co-IP of crosslinked Gimap3 was not. This might be explained by a too low protein concentration for antibodies to detect or the epitope recognized by anti-HA -antibody was occluded by proteins crosslinked with Gimap3, therefore preventing precipitation of proteins. Whether the shifted bands correspond to Gimap3 crosslinked to its interacting proteins or just protein aggregates, is not certain. Homobifunctional crosslinkers having only one reactive group increase the tendency to form intramolecular crosslinks in the same polypeptide or large protein aggregates, which could prevent the binding of the antibody (Fig. 12). Heterobifunctional crosslinkers with two different functional groups or crosslinkers with a short spacer arm could circumvent these problems (for review see Sinz, 2003). Crosslinkers with shorter spacer arms also prevent the formation of false positive interactions with proteins only localized close to the protein of interest but not really interacting *in vivo* (for review see Phizicky and Fields, 1995).

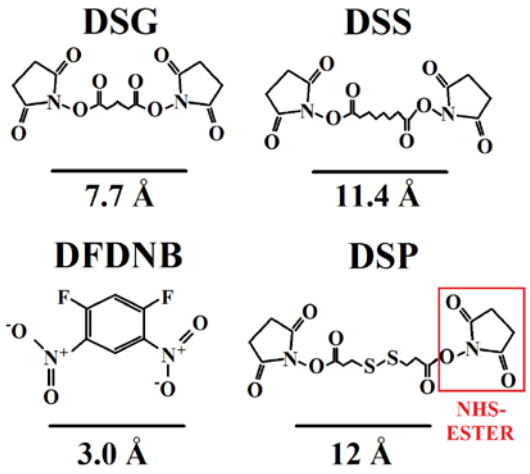

Figure 12: Chemical structures of crosslinkers in crosslinking experiments. DFDNB is an aryl halide with two reactive fluorine atoms, which form stable arylamine bonds. The only difference in the structure of NHS esters (DSG, DSS and DSP) is in the length of the hydrocarbon chain, the spacer arm, between two NHS esters (red rectangle). NHS esters react with the primary amines on the N-termini of peptides and also the ε-amine of lysine residues forming a stable, covalent amide and imide bonds. DSP is thiol-cleavable due to the sulphur bridge (S-S) in the hydrocardon chain and therefore its crosslink is the only reversible one. The length of the spacer arm of the crosslinker is presented under the black bar.

An alternative affinity-purification method for co-IP could be single-step Strep-tag purification. Instead of eluting the proteins by boiling, the tagged proteins could be

released by specific elution buffer. For example biotin in the elution buffer competes of the binding sites with the antibody, eluting specifically only the tagged proteins and proteins interacting with them. This way more transient and/or low-affinity protein interactions would be recovered, still having low level of background (Schmidt et al., 1996; Junttila et al., 2005).

5.1.4 Identification of interaction partners by mass spectrometry

Using only the transmembrane domain of Gimap3 for the identification of the interaction partners could explain the low number of prospective candidates found in the mass spectrometry experiment. As a transmembrane protein, Gimap3 was thought to interact via its C-terminal transmembrane domain rather than the N-terminal one. But as previous studies have shown, GIMAPs form homo –and hetero-oligomers in which the N-terminal G-domain and conserved box constitute an important part (Schwefel et al., 2010; Schwefel et al., 2013). As dimer form, GIMAPs are suggested to function as scaffolds and by preventing their dimerization, the interaction with other proteins could also be prevented (Schwefel et al., 2010; Schwefel et al., 2013). This could explain why Bcl-2 family members or the plausible new interaction partner Atg5 were not identified by mass spectrometry (Nitta et al., 2006; Schwefel et al., 2013). Besides stringent washes, transient protein interactions might have been missed because co-IP is biased towards protein interactions with high affinity and slow kinetics of dissociation. Protein tags as well as the diluted protein concentrations used in experiments, compared to highly concentrated macromolecule mixture in cells, can also hinder the affinities of transient protein interactions (Bray and Lay, 1997; for review see Berggård et al., 2007).

Protein interactions with Gimap3 could not be studied in their normal expression environment, T cells, due to the high level of background in the elution (Daheron et al., 2001; Jokinen et al., 2010). Nevertheless the wrong localization and interaction with false interaction partners were reduced by expressing *BALB Gimap3* constitutively and not by overexpression (Wong et al., 2010). Still, the post-translational modifications in

mammalian cells can affect the affinity of interacting proteins and biase the results (Daheron et al., 2001; for review see Berggård et al, 2007).

The interference with the detergent and its aggregates for proper peptide ionization was prevented by separating detergents from the sample using chromatography prior to electrospray ionization (Fenn et al., 1989; Beavis and Chait, 1990; for review see Yates, 1998). Nevertheless, either defective trypsin digestion due to non-existent cleavage site in proteins, missed cleavage site, or digestion into too small peptides, might have hindered the identification of peptides. These could explain why only the GFP-tag and not the transmembrane domain of Gimap3 was detected (Schirle et al., 2003). Also, simultaneous elution of same-sized peptides to the detector hinders the peptide identification (McCormack et al., 1997).

The protein identification by mass spectrometry is based on matching the experimental peptides mass, determined by their mass-to-charge ratio (*m/z*), with the candidate database sequences with allowed mass deviation and with specific enzyme cleavage site (McCormack et al., 1997; Perkins et al., 1999; Brosch et al., 2008). For each candidate, the specific algorithm of software, such as Mascot (Matrix Science), calculates a score indicating the quality of correlation of the two peptide fragmentation patterns and addresses the best match for the data (Perkins et al., 1999; Brosch et al., 2008). The probability-based scoring of Mascot is based on the probability that the observed match is a random event with a significance threshold for the probability to occur with a frequency below 5% ($p<0,05$) (Perkins et al., 1999). In other words the best match has the highest score but is not necessarily a significant one. Significance is presented by the exceptation value (E-value) indicating the number of matches with equal or better score that are expected to occur by chance alone: the lower the E-value the more significant the result (Brosch et al., 2008). Data quality also affects the significance. For example, there might not be enough mass values or the mass measurement accuracy is not good enough. Still, the best match might be correct although not significant. The significance of the match increases also with smaller databases used since the number of matches with the same score magnitude decreases (Perkins et al., 1999).

Determining the significance of mass spectrometry results is a difficult task. Peptides of abundant proteins, such as cytoskeletal proteins (keratin), chaperones and ribosomes, produce more peptides with strong signals, therefore dominating the mass spectrum and interfering with the peptide identification of proteins with low expression levels (McCormack et al., 1997; for review see Mann et al., 2001; Schirle et al., 2003; for review Berggård et al., 2007). This kind of unspecific background is difficult to completely eliminate, although the abundant proteins are not necessarily background in every case. These factors could partly explain the low score of the only interaction partner candidate in this study, SEC22b (App. 3). The interference of highly abundant proteins can be discriminated using databases, in which all the abundant core proteins of cell lines, such as HEK293 and HeLa, are listed to define the specifity of the interaction and rule out contaminations. This way also the false negatives (undetected real interaction) can be identified (Schirle et al., 2003).

Altogether, in this research a co-IP protocol for studying protein interactions of Gimap3 was optimized using 5µg of anti-HA antibody combined with DDM and high salt concentration washes. A 24 kDA SNARE protein, SEC22b, was found to interact with the transmembrane domain of Gimap3 but no evidence of interaction with Atg5 was found. All the results must be verified by repeating the experiments and performing co-IP against SEC22b. Interactions could be also confirmed by co-localization using fluorescence microscopy (for review see Phizicky and Fields, 1995; Cebrian et al., 2011). Whether Gimap3 has a role in antigen cross-presentation along with SEC22b needs to be determined (Mizushima et al., 2003; Cebrian et al., 2011). As N-terminus of Gimaps is essential for the oligomerization and possible protein binding, full-length Gimap3 should be used in further co-IP studies in order to identify more protein interactions (Schwefel et al., 2013). However the co-IP protocol needs to be optimized for the full-length Gimap3, especially in the reduction of background in elution. Discovering more protein interactions could clarify how Gimap3 modifies mtDNA segregation. Whether it would affect the fission machinery of mitochondria or interact with one of mammalian homolog of ERMES-like complex, as both are connected to the maintenance and segregation of mtDNA. Or could Gimap3 be a homolog of one of the ERMES proteins (Kornmann et al. 2009; Friedman et al. 2011; Murley et al., 2013)? Understanding how Gimap3 interacts

with Bcl-2 family members would also help to discover the mechanism by which Gimap3 and its homolog Gimap5 affect maturation of T cells (Daheron et al., 2001; Nitta et al., 2006; Schwefel et al., 2013; Yano et al., 2014).

6 REFERENCES

Aksoylar, H.I., K. Lampe, M. J. Barnes, D.R. Plas, and K. Hoebe. 2012. Loss of immunological tolerance in Gimap5-deficient mice is associated with loss of Foxo in CD4+ T cells. *J.Immunol.* 188:146-154.

Anderson, S., A.T. Bankier, B.G. Barrell, M.H.L. de Bruijn, A.R. Coulson, J. Drouin, I.C. Eperon, D.P. Nierlich, B.A. Roe, F. Sanger, P.H. Schreier, A.J.H. Smith, R. Staden, and I.G.Young. 1981. Sequence and organization of the human mitochondrial genome. *Nature.* 290:457-465.

Banerjee, P., J.B. Joo, J.T. Buse, and G. Dawson. 1995. Differential solubilization of lipids along with membrane proteins by different classes of detergents. *Chem.Phys.Lipids.* 77:65-78.

Barnes, M.J., H. Aksoylar, P. Krebs, T. Bourdeau, C.N. Arnold, Y. Xia, K. Khovananth, I. Engel, S. Sovath, K. Lampe, E. Laws, A. Saunders, G.W. Butcher, M. Kronenberg, K. Steinbrecher, D. Hildeman, H.L. Grimes, B. Beutler, and K. Hoebe. 2010. Loss of T cell and B cell quiescence precedes the onset of microbial flora-dependent wasting disease and intestinal inflammation in Gimap5-deficient mice. *J.Immunol.* 184:3743-3754.

Battersby, B.J., J.C. Loredo-Osti, and E.A. Shoubridge. 2003. Nuclear genetic control of mitochondrial DNA segregation. *Nat.Genet.* 33:183-186.

Battersby, B.J., M.E. Redpath, and E.A. Shoubridge. 2005. Mitochondrial DNA segregation in hematopoietic lineages does not depend on MHC presentation of mitochondrially encoded peptides. *Hum.Mol.Genet.* 14:2587-2594.

Battersby, B.J., and E.A. Shoubridge. 2001. Selection of a mtDNA sequence variant in hepatocytes of heteroplasmic mice is not due to differences in respiratory chain function or efficiency of replication. *Hum.Mol.Genet.* 10:2469-2479.

Beavis, R.C., and B.T. Chait. 1990. Rapid, sensitive analysis of protein mixtures by mass spectrometry. *Proc.Natl.Acad.Sci.U.S.A.* 87:6873-6877.

Berger, K.H., L.F. Sogo, and M.P. Yaffe. 1997. Mdm12p, a component required for mitochondrial inheritance that is conserved between budding and fission yeast. *J.Cell.Biol.* 136:545-553.

Berggård, T., S. Linse, and P. James. 2007. Methods for the detection and analysis of protein-protein interactions. *Proteomics.* 7:2833-2842.

Bleazard, W., J.M. McCaffery, E.J. King, S. Bale, A. Mozdy, Q. Tieu, J. Nunnari, and J.M. Shaw. 1999. The dynamin-related GTPase Dnm1 regulates mitochondrial fission in yeast. *Nat.Cell.Biol.* 1:298-304.

Boldogh, I., N. Vojtov, S. Karmon, and L.A Pon. 1998. Interaction between mitochondria and the actin cytoskeleton in budding yeast requires two integral mitochondrial outer membrane proteins, Mmm1p and Mdm10p. *J.Cell.Biol.* 141:1371-1381.

Boyman, O., C. Krieg, D. Homann, and J. Sprent. 2012. Homeostatic maintenance of T cells and natural killer cells. *Cell.Mol.Life.Sci.* 69:1597-1608.

Bray D., and S. Lay. 1997. Computer-based analysis of the binding steps in protein complex formation. *Proc.Natl.Acad.Sci.U.S.A.* 94:13493-13498.

Brosch, M., S. Swamy, T. Hubbard, and J. Choudhary. 2008. Comparison of Mascot and X! Tandem performance for low and high accuracy mass spectrometry and the development of an adjusted Mascot threshold. *Mol.Cell.Proteomics.* 7:962-970.

Bucher, M.H., A.G. Evdokimov, and D.S. Waugh. 2002. Differential effects of short affinity tags on the crystallization of *Pyrococcus furiosus* maltodextrin-binding protein. *Acta Crystallogr.D.Biol.Crystallogr.* 58:392-397.

Burgess, S.M., M. Delannoy, and R.E. Jensen. 1994. MMM1 encodes a mitochondrial outer membrane protein essential for establishing and maintaining the structure of yeast mitochondria. *J. Cell. Biol.* 126:1375-1391.

Cambot, M., S. Aresta, B. Kahn-Perlès, J. de Gunzburg, and P.H. Roméo. 2002. Human immune associated nucleotide 1: a member of a new guanosine triphosphatase family expressed in resting T and B cells. *Blood.* 99:3293-3301.

Cebrian, I., G. Visentin, N. Blanchard, M. Jouve, A. Bobard, C. Moita, J. Enninga, L.F. Moita, S. Amigorena, and A. Savina. 2011. Sec22b regulates phagosomal maturation and antigen crosspresentation by dendritic cells. *Cell.* 147:1355-1368.

Chinnery, P.F., and D.C. Samuels. 1999. Relaxed replication of mtDNA: A model with implications for the expression of disease. *Am.J.Hum.Genet.* 64:1158-1165.

Chinnery, P.F., P.J.G. Zwijnenburg, M. Walker, N. Howell, R.W. Taylor, R.N. Lightowlers, L. Bindoff, and Turnbull, D.M. 1999. Nonrandom tissue distribution of mutant mtDNA. *Am. J. Med. Genet.* 85:498-501.

Daheron, L., T. Zenz, L.D. Siracusa, C. Brenner, and B. Calabretta. 2001. Molecular cloning of Ian4: a BCR/ABL-induced gene that encodes an outer membrane mitochondrial protein with GTP-binding activity. *Nucleic Acids Res.* 29:1308-1316.

Dalberg, U., H. Markholst, and L. Hornum. 2007. Both Gimap5 and the diabetogenic BBDP allele of Gimap5 induce apoptosis in T cells. *Int. Immunol.* 19:447-53.

Dawid, I.B., and A.W. Blackler. 1972. Maternal and cytoplasmic inheritance of mitochondrial DNA in Xenopus. *Dev.Biol.* 29:152-161.

Dengjel, J., O. Schoor, R. Fischer, M. Reich, M. Kraus, M. Müller, K. Kreymborg, F. Altenberend, J. Brandenburg, H. Kalbacher, R. Brock, C. Driessen, H-G. Rammensee, and S. Stevanovic. 2005. Autophagy promotes MHC class II presentation of peptides from intracellular source proteins. *Proc.Natl.Acad.Sci.USA.* 102:7922-7927.

de Gunzburg, J., R. Riehl, and R.A. Weinberg. 1989. Identification of protein associated with p21ras by chemical crosslinking. *Proc.Natl.Acad.Sci.USA.* 86:4007-4011.

DiMauro, S., and E.A. Schon. 2003. Mitochondrial respiratory-chain diseases. *N.Engl.J.Med.* 348:2656-2668.

Dudley, E.C., H.T. Petrie, L.M. Shah, M.J. Owen, and A.C. Hayday. 1994. T cell receptor beta chain gene rearrangement and selection during thymocyte development in adult mice. *Immunity.* 1:83-93.

Dunbar, D.R., P.A. Moonie, H.T. Jacobs, and I.J. Holt. 1995. Different cellular backgrounds confer a marked advantage to either mutant or wild-type mitochondrial genomes. *Proc.Natl.Acad.Sci.USA.* 92:6562-6566.

Fenn, J.B., M. Mann, C.K. Meng, S.F. Wong, and C.M. Whitehouse. 1989. Electrospray ionization for mass spectrometry of large biomolecules. *Science.* 246:64-71.

Friedman, J.R., L.L. Lackner, M. West, J.R. DiBenedetto, J. Nunnari, and G.K. Voeltz. 2011. ER tubules mark sites of mitochondrial division. *Science.* 334:358-362.

Garavito, R.M., and S. Ferguson-Miller. 2001. Detergents as tools in membrane biochemistry. *J.Biol.Chem.* 276:32403-32406.

Garrido, N., L. Griparic, E. Jokitalo, J. Wartiovaara, A.M. van der Bliek, and J.N. Spelbrink. 2003. Composition and dynamics of human mitochondrial nucleoids. *Mol.Biol.Cell.* 14:1583-1596.

Gatto, L., J.A. Vizcaino, H. Hermjakob, W. Huber, and K.S. Lilley. 2010. Organelle proteomics experimental designs and analysis. *Proteomics.* 10:3957-3969.

Gerland, L.M., L. Genestier, S. Peyrol, M.C. Michallet, S. Hayette, I. Urbanowicz, P. Ffrench, J.P. Magaud, and M. Ffrench. 2004. Autolysosomes accumulate during in vitro CD8+ T-lymphocyte aging and may participate in induced death sensitization of senescent cells. *Exp.Gerontol.* 39:789-800.

Grossman, L.I., and E.A. Shoubridge. 1996. Mitochondrial genetics and human disease. *Bioessays.* 18:983-991.

Hall R.A. 2005. Co-immunoprecipitation as a strategy to evaluate receptor-receptor or receptor-protein interactions. In G-protein coupled receptor-protein interactions. George S.R., and Dowd B.F. editors. J*ohn Wiley & Sons Inc.* 165-178.

Hanekamp, T., M.K. Thorsness, I. Rebbapragagada, E.M. Fisher, C. Seebart, M.R. Darland, J.A. Coxbill, D.L. Updike, and P.E. Thorsness. 2002. Maintenance of mitochondrial morphology is linked to maintenance of the mitochondrial genome in Saccharomyces cerevisiae. *Genetics.* 162:1147-1156.

Hildeman, D.A., T. Mitchell, T.K. Teague, P. Henson, B.J. Day, J. Kappler, and P.C. Marrack. 1999. Reactive oxygen species regulate activation-induced T cell apoptosis. *Immunity.* 10:735-744.

Hill, K., K. Model, M.T. Ryan, K. Dietmeier, F. Martin, R. Wagner, and N. Pfanner. 1998. Tom40 forms the hydrophilic channel of the mitochondrial import pore for preproteins. *Nature.* 395:516-521.

Hobbs, A.E., M. Srinivasan, J.M. McCaffery, and R.E. Jensen. 2001. Mmm1p, a mitochondrial outer membrane protein, is connected to mitochondrial DNA (mtDNA) nucleoids and required for mtDNA stability. *J.Cell.Biol.* 152:401-410.

Holt, I.J., D.R. Dunbar, and H.T. Jacobs. 1997. Behaviour of a population of partially duplicated mitochondrial DNA molecules in cell culture: segregation, maintenance and recombination dependent upon nuclear background. *Hum.Mol.Genet.* 6:1251-1260.

Iborra, F.J., H. Kimura, and P.R. Cook. 2004. The functional organization of mitochondrial genomes in human cells. *BMC.Biol.* 2:9.

Jenuth, J.P., A.C. Peterson, and E.A. Shoubridge. 1997. Tissue-specific selection for different mtDNA genotypes in heteroplasmic mice. *Nat.Genet.* 16:93-95.

Jokinen, R., H. Junnila, and B.J. Battersby. 2011. Gimap3: A foot-in-the-door to tissue-specific regulation of mitochondrial DNA genetics. *Small GTPases.* 2:31-35.

Jokinen, R., P. Marttinen, H.K. Sandell, T. Manninen, H. Teerenhovi, T. Wai, D. Teoli, J.C. Loredo-Osti, E.A. Shoubridge, and B.J. Battersby. 2010. Gimap3 regulates tissue-specific mitochondrial DNA segregation. *PLoS Genet.* 6:e1001161.

Junttila, M.R., S. Saarinen, T. Schmidt, J. Kast, and J. Westermarck. 2005. Single-step Strep-tag purification for the isolation and identification of protein complexes from mammalian cells. *Proteomics.* 5:1199-1203.

Karbowski, M., K.L. Norris, M.M Cleland, S.Y. Jeong, and R.J. Youle. 2006. Role of Bax and Bak in mitochondrial morphogenesis. *Nature.* 443:658-662.

Kimura, M.Y., L.A. Pobezinsky, T.I. Guinter, J. Thomas, A. Adams, J.H. Park, X. Tai, and A. Singer. 2013. IL-7 signaling must be intermittent, not continuous, during $CD8^+$ T cell homeostasis to promote cell survival instead of cell death. *Nat.Immunol.* 14:143-151.

Kondylis, V., H.E. van Nispen tot Pannerden, S. van Dijk, T. Ten Broeke, R. Wubbolts, W.J. Geerts, C. Seinen, T. Mutis, and H.F.G. Heijnen. 2013. Endosome-mediated autophagy: an unconventional MIIC-driven autophagic pathway operational in dendritic cells. *Autophagy.* 9:861-880.

Kornmann, B., E. Currie, S.R. Collins, M. Schuldiner, J. Nunnari, J.S. Weissman, and P. Walter. 2009. An ER-mitochondria tethering complex revealed by a synthetic biology screen. *Science.* 325:477-481.

Kragh-Hansen, U., M. le-Maire, and J.V. Møller. 1998. The mechanism of detergent solubilization of liposomes and protein-containing membranes. *Biophys.J.* 75:2932-2946.

Krücken, J., R.M. Schroetel, I.U. Muller, N. Saidani, P. Marinovski, W.P. Benten, O. Stamm, and F. Wunderlich. 2004. Comparative analysis of the human gimap gene cluster encoding a novel GTPase family. *Gene.* 341:291-304.

le Maire, M., P. Champeil, and J.V. Møller. 2000. Interaction of membrane proteins and lipids with solubilizing detergents. *Biochim.Biophys.Acta.* 1508:86-111.

Lee, I., and W. Hong. 2006. Diverse membrane-associated proteins contain a novel SPM-domain. *FASEB J.* 20:202-206.

Lee, H.K., L.M. Mattei, B.E. Steinberg, P. Alberts, Y.H. Lee, A. Chervonsky, N. Mizushima, S. Grinstein, and A. Iwasaki. 2010. *In vivo* requirement for *Atg5* in antigen presentation by dendritic cells. *Immunity.* 32:227-239.

Lee, Y.H., H.T. Tan, and M.C. Chung. 2010. Subcellular fractionation methods and strategies for proteomics. *Proteomics.* 10:3935-3956.

Levine, B., and V. Deretic. 2007. Unveiling the roles of autophagy in innate and adaptive immunity. *Nat.Rev.Immunol.* 7:767-777.

Li, B., Z. Lei, B.D. Lichty, D. Li, G.M. Zhang, Z.H. Feng, Y. Wan, and B. Huang. 2009. Autophagy facilitates major histocompatibility complex class I expression induced by IFN-γ in B16 melanoma cells. *Cancer Immunol.Immunother.* 59:313-321.

MacMurray, A.J., D.H. Moralejo, A.E. Kwitek, E.A. Rutledge, B. Van Yserloo, P. Gohlke, S.J. Speros, B. Snyder, J. Schaefer, S. Bieg, J. Jiang, R.A. Ettinger, J. Fuller, T.L. Daniels, A. Pettersson, K. Orlebeke, B. Birren, H.J. Jacob, E.S. Lander, and A. Lernmark. 2002. Lymphopenia in the BB rat model of type 1 diabetes is due to a mutation in a novel immune-associated nucleotide (Ian)-related gene. *Genome Res.* 12:1029-1039.

Malena, A., E. Loro, M. Di Re, I.J. Holt, and L. Vergani. 2009. Inhibition of mitochondrial fission favours mutant over wild-type mitochondrial DNA. *Hum.Mol.Genet.* 18:3407-3416.

Mannella C.A., K. Buttle, B.K. Rath, and M. Marko. 1998. Electron microscopic tomography of rat-liver mitochondria and their interaction with the endoplasmic reticulum. *Biofactors.* 8:225-228.

Mann, M., R.C. Hendrickson, and A. Pandey. 2001. Analysis of proteins and proteomes by mass spectrometry. *Annu.Rev.Biochem.* 70:437-473.

McCormack, A.L., D.M. Schieltz, B. Goode, S. Yang, G. Barnes, D. Drubin, and J.R. Yates 3rd. 1997. Direct analysis and identification of proteins in mixtures by LC/MS/MS and database searching at the low-femtomole level. *Anal.Chem.* 69:767-776.

McLeod, I.X., W. Jia, and Y.W. He. 2012. The contribution of autophagy to lymphocyte survival and homeostasis. *Immunol.Rev.* 249:195-204.

Meeusen, S., and J. Nunnari. 2003. Evidence for a two membrane-spanning autonomous mitochondrial DNA replisome. *J.Cell.Biol.* 163:503-510.

Metz, S., C. Panke, A.K. Haas, J. Schanzer, W. Lau, R. Croasdale, E. Hoffmann, B. Schneider, J. Auer, C. Gassner, B. Bossenmaier, P. Umana, C. Sustmann, and U. Brinkmann. 2012. Bispecific antibody derivates with restricted binding functionalities that are activated by proteolytic processing. *Protein.Eng.Des.Sel.* 25:571-580.

Miyakawa, I., N. Sando, S. Kawano, S. Nakamura, and T. Kuroiwa. 1987. Isolation of morphologically intact mitochondrial nucleoids from the yeast, *Saccharomyces cerevisiae. J.Cell.Sci.* 88:431-439.

Mizushima, N., A. Kuma, Y. Kobayashi, A. Yamamoto, M. Matsubae, T. Takao, T. Natsume, Y. Ohsumi, and T. Yoshimori. 2003. Mouse Apg16L, a novel WD-repeat protein, targets to the autophagic isolation membrane with the Apg12-Apg5 conjugate. *J.Cell.Sci.* 116:1679-1688.

Murley, A., L.L. Lackner, C. Osman, M. West, G.K. Voeltz, P. Walter, and J. Nunnari. 2013. ER-associated mitochondrial division links the distribution of mitochondria and mitochondrial DNA in yeast. *Elife.* doi: 10.7554/eLife.00422.

Nedjic, J., M. Aichinger, J. Emmerich, N. Mizushima, and L. Klein. 2008. Autophagy in thymic epithelium shapes the T-cell repertoire and is essential for tolerance. *Nature.* 455:396-400.

Nitta, T., M. Nasreen, T. Seike, A. Goji, I. Ohigashi, T. Miyazaki, T. Ohta, M. Kanno, and Y. Takahama. 2006. IAN family critically regulates survival and development of T lymphocytes. *PLoS Biol.* 4:e103.

Nitta, T., and Y. Takahama. 2007. The lymphocyte guard-IANs: regulation of lymphocyte survival by IAN/GIMAP family proteins. *Trends Immunol.* 28:58-65.

Nunnari, J., W.F. Marshall, A. Straight, A. Murray, J.W. Sedat, and P. Walter. 1997. Mitochondrial transmission during mating in Saccharomyces cerevisiae is determined by mitochondrial fusion and fission and the intramitochondrial segregation of mitochondrial DNA. *Mol.Biol.Cell.* 8:1233-1242.

Ou, W.J., J.J. Bergeron, Y. Li, C.Y. Kang, and D.Y. Thomas. 1995. Conformational changes induced in the endoplasmic reticulum luminal domain of calnexin by Mg-ATP and Ca2+. *J.Biol.Chem.* 270:18051-18059.

Perkins, D.N., D.J. Pappin, D.M. Creasy, and J.S. Cottrell. 1999. Probability-based protein identification by searching sequence databases using mass spectrometry data. *Electrophoresis.* 20:3551-3567.

Phizicky, E.M., and S. Fields. 1995. Protein-protein interactions: methods for detection and analysis. *Microbiol.Rev.* 59:94-123.

Poirier, G.M., G. Anderson, A. Huvar, P.C. Wagaman, J. Shuttleworth, E. Jenkinson, M.R. Jackson, P.A. Peterson, and M.G. Erlander. 1999. Immune-associated nucleotide-1 (IAN-1) is a thymic selection marker and defines a novel gene family conserved in plants. *J.Immunol.* 163:4960-4969.

Pua, H.H., I. Dzhagalov, M. Chuck, N. Mizushima, and Y.W. He. 2007. A critical role for the autophagy gene Atg5 in T cell survival and proliferation. *J.Exp.Med.* 204:25-31.

Reuber, T.L., and F.M. Ausubel. 1996. Isolation of Arabidopsis genes that differentiate between resistance responses mediated by the RPS2 and RPM1 disease resistance genes. *Plant Cell.* 8:241-249.

Rossignol, R., R. Gilkerson, R. Aggeler, K. Yamagata, S.J. Remington, and R.A. Capaldi. 2004. Energy substrate modulates mitochondrial structure and oxidative capacity in cancer cells. *Cancer Res.* 64:985-993.

Sandal T., L. Aumo, L. Hedin, B.T. Gjertsen, and S.O. Doskeland. 2003. Irod/Ian5: an inhibitor of gamma-radiation- and okadaic acid-induced apoptosis. *Mol. Biol. Cell.* 14:3292-304.

Satoh, M., and T. Kuroiwa. 1991. Organization of multiple nucleoids and DNA molecules in mitochondria of a human cell. *Exp.Cell.Res.* 196:137-140.

Schirle, M., M.A. Heurtier, and B.Kuster. 2003. Profiling core proteomes of human cell lines by one-dimensional PAGE and liquid chromatography-tandem mass spectrometry. *Mol.Cell.Proteomics.* 2:1297-1305.

Schmid, D., M. Pypaert, and C. Münz. 2007. Antigen-loading compartments for major histocompatibility complex class II molecules continually receive input from autophagosomes. *Immunity.* 26:79-92

Schmidt, T.G., J. Koepke, R. Frank, and A. Skerra. 1996. Molecular interaction between the Strep-tag affinity peptide and its cognate target, streptavidin. *J.Mol.Biol.* 255:753-766.

Schnell, S., C. Démollière, P. van den Berk, and H. Jacobs. 2006. Gimap4 accelerates T-cell death. *Blood.* 108:591-599.

Schulteis, R.D., H. Chu, X. Dai., Y. Chen, B. Edwards, D. Haribhai, C.B. Williams, S. Malarkannan, M.J. Hessner, S. Glisic-Milosavljevic, S. Jana, E.J. Kerschen, S. Ghosh, D. Wang, A.E. Kwitek, A. Lernmark, J. Gorski, and H. Weiler. 2008. Impaired survival of peripheral T cells, disrupted NK/NK T cell development, and liver failure in mice lacking Gimap5. *Blood.* 112:4905-4914.

Schwefel, D., B.S. Arasu, S.F. Marino, B. Lamprecht, K. Köchert, E. Rosenbaum, J. Eichhorst, B. Wiesner, J. Behlke, O. Rocks, S. Mathas, and O. Daumke. 2013. Structural insights into the mechanism of GTPase activation in the GIMAP family. *Structure.* 21:550-559.

Schwefel, D., C. Frohlich, J. Eichhorst, B. Wiesner, J. Behlke, L. Aravind, and O. Daumke. 2010. Structural basis of oligomerization in septin-like GTPase of immunity-associated protein 2 (GIMAP2). *Proc.Natl.Acad.Sci.U.S.A.* 107:20299-20304.

Seddon, A.M., P. Curnow, and P.J. Booth. 2004. Membrane proteins, lipids and detergents: not just a soap opera. *Biochim.Biophys.Acta.* 1666:105-117.

Sinz, A. 2003. Chemical cross-linking and mass spectrometry for mapping three-dimensional structures of proteins and protein complexes. *J. Mass Spectrom.* 38:1225-1237.

Smirnova, E., L. Griparic, D.L. Shurland, and A.M. van der Bliek. 2001. Dynamin-related protein Drp1 is required for mitochondrial division in mammalian cells. *Mol.Biol.Cell.* 12:2245-2256.

Sogo, L.F. and M.P. Yaffe. 1994. Regulation of mitochondrial morphology and inheritance by Mdm10p, a protein of the mitochondrial outer membrane. *J.Cell.Biol.* 126:1361-1373.

Taylor, R.W., and D.M. Turnbull. 2005. Mitochondrial DNA mutations in human disease. *Nat.Rev.Genet.* 6:389-402.

Tomoda, K., Y. Kubota, Y. Arata, S. Mori, M. Maeda, T. Tanaka, M. Yoshida, N. Yoneda-Kato, and J.Y. Kato. 2002. The cytoplasmic shuttling and subsequent degradation of p27Kip1 mediated by Jab1/CSN5 and the COP9 signalosome complex. *J.Biol.Chem.* 277:2302-2310.

Toulmay, A., and W.A. Prinz. 2012. A conserved membrane-binding domain targets proteins to organelle contact sites. *J.Cell.Sci.* 125:49-58.

Veis, D.J., C.L. Sentman, E.A. Bach, and S.J. Korsmeyer. 1993. Expression of the Bcl-2 protein in murine and human thymocytes and in peripheral T lymphocytes. *J.Immunol.* 151:2546-2554.

von Boehmer, H., I. Aifantis, J. Feinberg, O. Lechner, C. Saint-Ruf, U. Walter, J. Buer, and O. Azoqui. 1999. Pleiotropic changes controlled by the pre-T-cell receptor. *Curr.Opin.Immunol.* 11:135-142.

Walsh, C.M., and A.L. Edinger. 2010. The complex interplay between autophagy, apoptosis, and necrotic signals promotes T-cell homeostasis. *Immunol.Rev.* 236:95-109.

Weber, K., J.N. Wilson, L. Taylor, E. Brierley, M.A. Johnson, D.M. Turnbull, and L.A. Bindoff. 1997. A new mtDNA mutation showing accumulation with time and restriction to skeletal muscle. *Am.J.Hum.Genet.* 60:373-380.

Wong, V.W., A.E. Saunders, A. Hutchings, J.C. Pascall, C. Carter, N.A. Bright, S.A. Walker, N.T. Ktistakis, and G.W. Butcher. 2010. The autoimmunity-related GIMAP5 GTPase is a lysosome-associated protein. *Self Nonself.* 1:259-268.

Xu, X., S. Zhang, P. Li, J. Lu, Q. Xuan, and Q. Ge. 2013. Maturation and emigration of single-positive thymocytes. *Clin.Dev.Immunol.* doi: 10.1155/2013/282870.

Yano K., C. Carter, N. Yoshida, T. Abe, A. Yamada, T. Nitta, N. Ishimaru, K. Takada, G.W. Butcher, Y. Takahama. 2014. Gimap3 and Gimap5 cooperate to maintain T-cell numbers in mouse. *Eur.J.Immunol.* 44:561-572.

Yates, J.R 3rd. 1998. Mass spectrometry and the age of the proteome. *J.Mass.Spectrom.* 33:1-19.

Zenz, T., A. Roessner, A. Thomas, S. Frohling, H. Dohner, B. Calabretta, and L. Daheron. 2004. hIan5: the human ortholog to the rat Ian4/Iddm1/lyp is a new member of the Ian family that is overexpressed in B-cell lymphoid malignancies. *Genes Immun.* 5:109-116.

APPENDICES

Appendix 1: Antibodies used in the experiments.

PRIMARY ANTIBODIES (monoclonal=M, polyclonal=P, source specie)	DILUTION (immuno-blot)	TARGET SIZE (kDA)	MANUFACTURER
Calnexin (rabbit)	1:1000	90	Assay designs
Tom40 (P, rabbit)	(1:2000)	40	SANTA CRUZ BIOTECHNOLOGY
SGN5 (=COPS5) (mouse)	1:1000		BD Transduction Laboratories
Anti-Atg5 (C-terminal, rabbit)	1:1000	56	SIGMA®
GFP=3H9 (M, rat)	1:1000		Chromotek
Anti c-myc (M, mouse)	1:1000		Roche
Gimap3 (Balb sera IgG enriched, rabbit)	1:1000	34	BioGENES

SECONDARY ANTIBODIES	DILUTION	MANUFACTURER
Peroxidase-conjugated AffiniPure Goat Anti-Rabbit IgG (H+L) (goat)	1: 20 000	Jackson ImmunoResearch LABORATORIES Inc
Peroxidase-conjugated AffiniPure Goat Anti-Mouse IgG (H+L) (goat)	1: 10 000	Jackson ImmunoResearch LABORATORIES Inc.
Biotinylated Anti-Rat IgG (H+L) (rabbit)	1: 20 000	VECTOR LABORATORIES

Appendix 2: Buffers used in each experiment

BUFFER	PROTOCOL	CONTENT
HIM buffer pH adjusted to 7.5 with 1 M KOH	3.2, 3.7	200 mM D-mannitol (SIGMA-ALDRICH) 70 mM Sucrose (S0389, SIGMA-ALDRICH) 10 mM HEPES (H3375, SIGMA-ALDRICH) 1 mM Ethylene glycol-bis(beta-aminoethyl ether)-N,N,N´,N´,-tetra acetic acid (EGTA, Amresco)
1x Phosphate buffered saline (1xPBS) pH 7.4	3.3	0,01 M phosphate buffer 0,0027 M Kcl 0,140 M NaCl PBS-tablet (Medicago) solved to 1 liter of water
Lysis buffer I	3.3 (4.1)	50 mM KPO_4 (pH 7.6) 150 mM NaCl 1 mM Phenylmethanesulfonyl fluoride solution (PMSF, FLUKA) 1% *n*-Dodecyl β-D-maltoside (DDM, Amresco)
Wash buffer I	3.3 (4.1)	50 mM KPO_4 (pH7.6) 150 mM NaCl 1 mM PMSF 0,1% DDM (Amresco)
Lysis buffer II	3.3	1xPBS (140 mM NaCl) pH 7.4 1 mM PMSF 1% detergent: -DDM (Amresco) (4.3, 4.4) -Sodium taurodeoxycholate (SIGMA-ALDRICH) (4.2-4.5.1) -Octyl-β-D-Glucopyranoside (SIGMA-ALDRICH) (4.3) -Digitonin (SIGMA-ALDRICH) (4.3)
Wash buffer II	3.3	1xPBS (low: 140 / high: 400 mM NaCl) pH 7.4 1 mM PMSF 0,1% detergent: -DDM (4.3, 4.4) -Sodium taurodeoxycholate (4.2-4.5.1) -Octyl-β-D-Glucopyranoside (4.3) -Digitonin (4.3)
Bradford protein assay dye	3.3, 3.5	Bio-Rad Protein Assay Dye Reagent Concentrate (BIO-RAD) was diluted 1:10 into MQ water

2xLaemmli buffer (stock) pH 6.8	3.3, 3.5	4% (v/v) SDS 20% (v/v) glycerol 0.12 M Tris-HCl 0.01% (v/v) bromophenol blue
1xLaemmli buffer pH 6.8	3.3, 3.5	50% (v/v) 2x laemmli stock 45% (v/v) H_2O 5% (v/v) β-mercaptoethanol
TG-SDS (Amresco) pH 8.5	3.5	25 mM Tris base 192 mM glycine 0.1% SDS
Semi-dry transfer buffer pH 8.3	3.5	39 mM glycine 48 mM Tris base 0.075% (v/v) SDS 20% (v/v) methanol
10x TBS	3.5	200 mM Tris base 1370 mM NaCl
1x TBST	3.5	Add 0.1% (v/v) Tween-20 to 1x TBS
Fix solution	3.5	30% Ethanol (ETAX, Altia Oyj) 10% acetic acid (Fluka) 60% MQ water
Wash solution (silverstain)	3.5	100% ethanol was diluted 1:10 into MQ water
Stop solution	3.5	100% Acetic acid was diluted 1:20 into MQ water
0,5 M glycine (pH 8.0)	3	0,5 % (v/v) glycine (SIGMA-ALDRICH) solved into MQ water pH adjusted with 5M and 1M NaOH

Appendix 3: Identified proteins from co- IP elution of GFP-(261-301)Gimap3 by mass spectrometry.

Brown=found also in control co-IP, red= putative interacting candidate, green=GFP-tag

ELUTION WITH ANTI-HA ANTIBODY			
SWISSPROT ID	**NAME OF PROTEIN**	**SCORE**	**QUERIES MATCHED**
P04264|K2C1_HUMAN	Keratin, type II cytoskeletal 1	2432	77
P35527|K1C9_HUMAN	Keratin, type I cytoskeletal 9	1944	68
P35908|K22E_HUMAN	Keratin, type II cytoskeletal 2 epidermal	1758	65
P13645|K1C10_HUMAN	Keratin, type I cytoskeletal 10	1753	50
Q5R8F7|PABP1_PONAB	Polyadenylate-binding protein 1	752	40
Q3U0V1|FUBP2_MOUSE	Far upstream element-binding protein 2	710	31
P04259|K2C6B_HUMAN	Keratin, type II cytoskeletal 6B	695	27
P48668|K2C6C_HUMAN	Keratin, type Ii cytoskeletal 6C	694	28
P00761|TRYP_PIG	Trypsin	667	33
P02538|K2C6A_HUMAN	Keratin, type II cytoskeletal 6A	662	27
P13647|K2C5_HUMAN	Keratin, type II cytoskeletal 5	574	26
Q13310|PABP4_HUMAN	Polyadenylate-binding protein 4	532	18
A2Q0Z0|EF1A1_HORSE	Elongation factor 1-alpha 1	389	19
Q0VCX2|GRP78_BOVIN	78 kDA glucose-regulated protein	363	10
Q91883|GRP78_XENLA	78 kDA glucose-regulated protein	305	9
Q9Z1E1|FLOT1_RAT	Flotillin-1	303	8
Q8UVD9|FUBP2_CHICK	Far upstream element-binding protein 2	284	18
P31025|LCN1_HUMAN	Lipocalin-1	276	12
P02533|K1C14_HUMAN	Keratin, type I cytoskeletal 14	248	14
P61626|LYSC_HUMAN20	Lysozyme C	233	8
P08779|K1C16_HUMAN	Keratin, type I cytoskeletal 16	208	13
Q3U962|CO5A2_MOUSE	Collagen alpha-2 (V) chain	194	10
P02663|CASA2_BOVIN	Alpha-S2-casein	191	13
Q5RBS3|SERPH_PONAB	Serpin H1	174	3
Q8WX93|PALLD_HUMAN	Palladin	171	6
Q9Z2S9|FLOT2_RAT	Flotillin-2	150	11
P11087|CO1A1_MOUSE	Collagen alpha-1 (I) chain	144	13
Q3T0D0|HNRPK_BOVIN	Heterogeneous nuclear ribonucleoprotein K	136	7
Q91WJ8|FUBP1_MOUSE	Far upstream element-binding protein 1	134	10
O95678|K2C75_HUMAN	Keratin, type II cytoskeletal 75	133	7
P01868|IGHG1_MOUSE	Ig gamma-1 chain C region secreted form	130	4
Q60847|COCA1_MOUSE	Collagen alpha-1(XII) chain	130	14
Q7Z794|K2C1B_HUMAN	Keratin, type II cytoskeletal 1b	130	8
A2Q0Z1|HSP7C_HORSE	Heat shock cognate 71 kDa protein	117	6

A2V9Z4|ALBU_MACFA	Serum albumin	117	3
P42212|GFP_AEQVI	Green fluorescent protein	107	6
P02754|LACB_BOVIN	Beta-lactoglobulin	102	3
Q8VIJ6|SFPQ_MOUSE	Splicing factor, proline-and glutamine-rich	95	5
A2BDB0|ACTG_XENLA	Actin, cytoplasmic 2	85	4
Q0P5J4|K1C25_BOVIN 40	Keratin, type I cytoskeletal 25	82	8
Q9D554|SF3A3_MOUSE	Splicing factor 3A subunit 3	80	2
Q5R7W2|MPCP_PONAB	Phosphate carrier protein, mitochondrial	80	1
P02662|CASA1_BOVIN	Alpha-S1-casein	78	5
Q15717|ELAV1_HUMAN	ELAV-like protein 1	78	2
Q7TQH0|ATX2L_MOUSE	Ataxin-2-like protein	77	2
P0AA25|THIO_ECOLI	Thioredoxin-1	77	2
P02668|CASK_BOVIN	Kappa-casein	77	3
Q9GZZ8|LACRT_HUMAN	Extracellular glycoprotein lacritin	68	3
P05109|S10A8_HUMAN	Protein S100-A8	67	3
P62318|SMD3_HUMAN	Small nuclear ribonucleoprotein Sm D3	61	1
P02788|TRFL_HUMAN	Lactotransferrin	60	6
Q5RA31|TOM20_PONAB	Mitochondrial import receptor subunit TOM20 homolog	58	1
A1XQR9|RUXE_PIG	Small nuclear ribonucleoprotein E	56	1
Q1LZB6|CAPR1_BOVIN	Caprin-1	56	2
Q7TSC1|PRC2A_MOUSE	Protein PRRC2A	55	1
Q5FVM4|NONO_RAT	Non-POU domain-containing octamer-binding protein	53	3
Q61072|ADAM9_MOUSE	Disintegrin and metalloproteinase domain-containing protein 9	52	1
Q05793|PGBM_MOUSE	Basement membrane-specific heparan sulfate proteoglycan core protein	52	5
Q5IS70|ATN1_PANTR	Atrophin-1	51	1
Q3T0V3|EIF3K_BOVIN 60	Eukaryotic translation initiation factor 3 subunit K	48	1
B3MLB7|AFF4_DROAN	AF4/FMR2 family member 4	48	1
P67975|LACB_OVIMU	Beta-lactoglobulin	48	2
Q01149|CO1A2_MOUSE	Collagen alpha-2(I) chain	46	2
Q4KM74|SC22B_RAT	Vesicle-trafficking protein SEC22b	45	1
P35394|TBB_ENTDO	Tubulin beta chain	45	2
P09207|TBB6_CHICK	Tubulin beta-6 chain	45	2
A1WWU7|SYS_HALHL	Seryl-tRNA synthetase	45	2
B5FA11|DNAK_VIBFM	Chaperone protein DnaK	41	3
Q9JLV1|BAG3_MOUSE	BAG family molecular chaperone regulator 3	41	3

Blue= fragments of the mouse IgG antibody used as control co-IP antibody.

ELUTION WITH MOUSE IgG CONTROL ANTIBODY			
SWISSPROT ID	**NAME OF PROTEIN**	**SCORE**	**QUERIES MATCHED**
P04264|K2C1_HUMAN	Keratin, type II cytoskeletal 1	1881	55
P35527|K1C9_HUMAN	Keratin, type I cytoskeletal 9	1449	46
P13538|MYSS_CHICK	Myosin heavy chain, skeletal muscle, adult	1270	55
P01868|IGHG1_MOUSE	Ig gamma-1 chain C region secreted form	1238	82
P35908|K22E_HUMAN	Keratin, type II cytoskeletal 2 epidermal	1201	42
P13645|K1C10_HUMAN	Keratin, type I cytoskeletal 10	1030	36
P01863|GCAA_MOUSE	Ig gamma-2A chain C region, A allele	872	56
P00761|TRYP_PIG	Trypsin	860	39
P01864|GCAB_MOUSE	Ig gamma-2A chain C region secreted form	762	36
P01837|IGKC_MOUSE	Ig kappa chain C region	605	49
P02565|MYH3_CHICK	Myosin-3	477	22
P06330|HVM51_MOUSE	Ig heavy chain V region AC38 205.12	441	14
Q5R9Q5|ACTS_PONAB	Actin, alpha skeletal muscle	422	19
O35501|GRP75_CRIGR	Stress-70 protein, mitochondrial	394	19
P28798|GRN_MOUSE	Granulins	274	10
P13647|K2C5_HUMAN	Keratin, type II cytoskeletal 5	257	13
Q0VCX2|GRP78_BOVIN	78 kDa glucose-regulated protein	250	9
P35441|TSP1_MOUSE	Thrombospondin-1	243	12
P01631|KV2A7_MOUSE	Ig kappa chain V-II region 26-10	231	6
P04259|K2C6B_HUMAN	Keratin, type II cytoskeletal 6B	216	15
P01636|KV5A4_MOUSE	Ig kappa chain V-V region MOPC 149	214	4
A5A6I5|ALDOA_PANTR	Fructose-bisphosphate aldolase A	208	8
P31025|LCN1_HUMAN	Lipocalin-1	197	7
P04268|TPM1_CHICK	Tropomyosin alpha-1 chain	174	6
P01654|KV3A1_MOUSE	Ig kappa chain V-III region PC 2880/PC 1229	166	3
P01635|KV5A3_MOUSE	Ig kappa chain V-V region K2 (Fragment)	160	10
P01659|KV3A7_MOUSE	Ig kappa chain V-III region TEPC 124	158	4
P01670|KV3AI_MOUSE	Ig kappa chain V-III region PC 6684	157	4
P84751|HVM63_MOUSE	Ig heavy chain Mem5 (Fragment)	149	8
P01746|HVM02_MOUSE	Ig heavy chain V region 93G7	146	2
P02538|K2C6A_HUMAN	Keratin, type II cytoskeletal 6A	146	12
P01639|KV5A7_MOUSE	Ig kappa chain V-V region	142	3

	MOPC 41		
P01605|KV113_HUMAN	Ig kappa chain V-I region Lay	135	5
P00356|G3P_CHICK	Glyceraldehyde-3-phosphate dehydrogenase	128	6
P00340|LDHA_CHICK	L-lactate dehydrogenase A chain	125	6
P04945|KV6AB_MOUSE	Ig kappa chain V-VI region NQ2-6.1	125	1
P61626|LYSC_HUMAN	Lysozyme C	124	4
P00548|KPYK_CHICK	Pyruvate kinase muscle isozyme	122	6
P07322|ENOB_CHICK	Beta-enolase	119	4
P18531|HVM60_MOUSE	Ig heavy chain V region M315	119	2
P01644|KV5AB_MOUSE	Ig kappa chain V-V region HP R16.7	118	10
P02533|K1C14_HUMAN	Keratin, type I cytoskeletal 14	111	6
P00565|KCRM_CHICK	Creatine kinase M-type	110	6
P01674|KV3AM_MOUSE	Ig kappa chain V-III region PC 2154	107	4
P06398|TNNT3_COTJA	Troponin T, fast skeletal muscle isoforms	107	1
P01618|KV1_CANFA	Ig kappa chain V region GOM	99	1
P01843|LAC1_MOUSE	Ig lambda-1 chain C region	98	2
P08779|K1C16_HUMAN	Keratin, type I cytoskeletal 16	98	7
P02604|MLE1_CHICK	Myosin light chain 1, skeletal muscle isoform	92	3
P01657|KV3A5_MOUSE	Ig kappa chain V-III region PC 2413	89	4
P01796|HVM27_MOUSE	Ig heavy chain V-III region A4	89	4
P02662|CASA1_BOVIN	Alpha-S1-casein	88	5
P01675|KV6A1_MOUSE	Ig kappa chain V-VI region XRPC 44	86	1
P00940|TPIS_CHICK	Triosephosphate isomerase	86	4
P03976|KV2A5_MOUSE	Ig kappa chain V-II region 17S29.1	86	1
P01642|KV5A9_MOUSE	Ig kappa chain V-V region L7 (Fragment)	84	2
P06654|SPG1_STRSG	Immunoglobulin G-binding protein G	83	3
P01680|KV4A1_MOUSE	Ig kappa chain V-IV region S107B	82	2
P01630|KV2A6_MOUSE	Ig kappa chain V-II region 7S34.1	82	1
Q9WUU7|CATZ_MOUSE	Cathepsin Z	81	6
P02769|ALBU_BOVIN	Serum albumin	78	6
A2V9Z4|ALBU_MACFA	Serum albumin	78	5
P02754|LACB_BOVIN	Beta-lactoglobulin	77	3
O75955|FLOT1_HUMAN	Flotillin-1	74	5
P01633|KV5A1_MOUSE	Ig kappa chain V19-17	74	4
P51903|PGK_CHICK	Phosphoglycerate kinase	74	2
P07309|TTHY_MOUSE	Transthyretin	72	1
P01662|KV3AA_MOUSE	Ig kappa chain V-III region ABPC 22/PC 9245	71	1

Q2KJD0|TBB5_BOVIN	Tubulin beta-5 chain	68	2
Q3ZC55|ACTN2_BOVIN	Alpha-actinin-2	67	1
P01638|KV5A6_MOUSE	Ig kappa chain V-V region L6 (Fragment)	66	3
P02668|CASK_BOVIN	Kappa-casein	65	2
P05109|S10A8_HUMAN	Protein S100-A8	65	1
P0AA25|THIO_ECOLI	Thioredoxin-1	64	2
P01806|HVM36_MOUSE	Ig heavy chain V region 441	63	4
Q3U0V1|FUBP2_MOUSE	Far upstream element-binding protein 2	62	3
P16419|MYPC2_CHICK	Myosin-binding protein C, fast-type	62	4
P05081|KAD1_CHICK	Adenylate kinase isoenzyme 1	62	2
Q66HD0|ENPL_RAT	Endoplasmin	60	2
P13585|AT2A1_CHICK	Sarcoplasmic/endoplasmic reticulum calcium ATPase 1	57	2
P05063|ALDOC_MOUSE	Fructose-bisphosphate aldolase C	54	2
P18524|HVM53_MOUSE	Ig heavy chain V region RF	53	3
P01786|HVM17_MOUSE	Ig heavy chain V region MOPC 47A	52	2
P0CN30|EF1A_CRYNJ	Elongation factor 1-alpha	51	1
P01783|HVM16_MOUSE	Ig heavy chain V region MOPC 21 (Fragment)	49	2
P01625|KV402_HUMAN	Ig kappa chain V-IV region Len	49	3
P01750|HVM06_MOUSE	Ig heavy chain V region 102	47	1
P40851|AXL1_YEAST	Putative protease AXL1	47	6
P02663|CASA2_BOVIN	Alpha-S2-casein	45	2
Q2HJ60|ROA2_BOVIN	Heterogeneous nuclear ribonucleoproteins A2/B1	44	2
Q0P5J4|K1C25_BOVIN	Keratin, type I cytoskeletal 25	44	3
Q5E9A3|PCBP1_BOVIN	Poly(rC)-binding protein 1	43	1
Q8D3I8|OXAA_WIGBR	Membrane protein oxaA	42	1
P02788|TRFL_HUMAN	Lactotransferrin	42	2
O67087|SYFA_AQUAE	Phenylalanyl-tRNA synthetase alpha chain	42	1
C0PWW0|GPMA_SALPC	2,3-bisphosphoglycerate-dependent phosphoglycerate mutase	42	1
Q01008|VP23_SHV21	Triplex capsid protein 26	42	2